国際化推進共同研究概要

No. 1

タイトル： Magnetic stirring in crystal growth and solidification of materials with different electrical conductivity.

研究代表者：DROPKA, Natasa

所内世話人：柿本　浩一

期　間：　2012年1月15日～1月19日

研究概要：　太陽電池用シリコン結晶の成長プロセスに関して、電磁攪拌法を用いた新規方法の提案を行った。
特に、太陽電池の特性を作用する不純物である酸素、炭素等の濃度低減を加熱用高周波電力の位相、周波数を変化により可能とする新規方法に関する討論等の打ち合わせを行った。今後も、継続的に共同研究を継続する。

International Joint Research Report for 2011

Subject field: Renewable Energy Dynamics
Subtheme: Magnetic stirring in crystal growth and solidification of materials with different electrical conductivity
RIAM attendant: Professor Dr. K. Kakimoto
Representative person: Dr. N. Dropka
Co-researchers: Dr. Ch. Frank-Rotsch, Dr. W. Miller, U. Rehse

Aim of the joint research project between Research Institute for Applied Mechanics (RIAM), Kyushu University in Fukuoka and Leibniz Institute for Crystal Growth (IKZ) in Berlin was to cooperate in studying the application of unsteady magnetic fields for improved stirring and interface shaping during crystal growth of materials that vary in their electrical conductivity in the wide range, from 10^2 Sm^{-1} up to 10^6 Sm^{-1} (Table 1). For this purpose, different Vertical Gradient Freeze (VGF) crystal growth configurations were considered.

Table 1. Material properties relevant for crystal growth.

	state	Ge	Si	BaF_2	CdTe	YAG
λ [W/mK]	melt	39	67	0,2	3	4
	solid	17	22	2	1,5	8
ΔH_{LS} [J/m^3]		$4 \cdot 10^9$	$4{,}6 \cdot 10^9$	$1{,}8 \cdot 10^9$	$1{,}3 \cdot 10^9$	$1{,}96 \cdot 10^9$
σ_{el} [S/m]	melt	$1{,}7 \cdot 10^6$	$1{,}2 \cdot 10^6$	392	$1{,}05 \cdot 10^4$	600
	solid	$1{,}6 \cdot 10^6$	$5 \cdot 10^4$	392	$8{,}5 \cdot 10^3$	5
ν [m^2/s]	melt	$1{,}4 \cdot 10^{-7}$	$3{,}4 \cdot 10^{-7}$	$2{,}48 \cdot 10^{-6}$	$4{,}5 \cdot 10^{-7}$	$1{,}3 \cdot 10^{-5}$
α [K^{-1}]	melt	$1{,}1 \cdot 10^{-4}$	$1{,}1 \cdot 10^{-4}$	$2 \cdot 10^{-5}$	$1{,}45 \cdot 10^{-4}$	$1{,}8 \cdot 10^{-5}$
ρ [kg/m^3]	melt	5500	2530	4830	5640	4300

The feasibility of a Travelling Magnetic Field (TMF) for improved stirring and interface shaping was shown in a recently published paper (N. Dropka et al.,J. Cryst. Growth 338 (2012), 208). Numerical studies were focused on the interface shaping during crystal growth of Ge, Si, CdTe, YAG and BaF2 using Travelling Magnetic Fields (TMFs) generated in a KRIST*MAG*® heater magnet module. The results showed that Lorentz force densities comparable or larger than the buoyancy force densities can be achieved by using moderate electrical currents. For materials with small electrical conductivity, to keep the current magnitude low, higher frequencies should be used (Figure 1). Positive deflection was obtained using downward directed TMFs for all studied materials. An example of the flow pattern and interface morphology for CdTe grown in different regimes: i) pure buoyancy, ii) upwards and iii) downwards TMF was depicted in Figure 2.
Additionally to interface shaping, stirring potential of TMF and Carousel magnetic fields (CMF) in crystal growth and solidification of mc-silicon for PV was investigated. Favorable flow distributions for enhanced process purity can be achieved by tailoring the flow with one or combined mono- and double-frequency TMF and CMF. The optimal Lorentz force density distribution represents intrinsic property of each set-up, i.e. its design and selected process parameters.
The obtained numerical results were presented at "Free discussion meeting for crystal growth" that was organized and hosted by RIAM attendant Professor Dr. K. Kakimoto at Research Institute for Applied Mechanics, Kyushu University, on 17.-18.01.2012. The main focus of the meeting was crystal growth of Si and SiC. The contribution reflecting RIAM-IKZ cooperation was: N. Dropka et

al.,"Analysis for crystal growth mechanism". These results were widely discussed with Prof. Kakimoto, his team, and other participants – finally also in direction towards possible future cooperation. The visit of Professor Kakimoto's lab that followed the meeting and discussion with him, his team and other participants of the workshop was very fruitful and gave a better insight into the complexity of the phenomena.

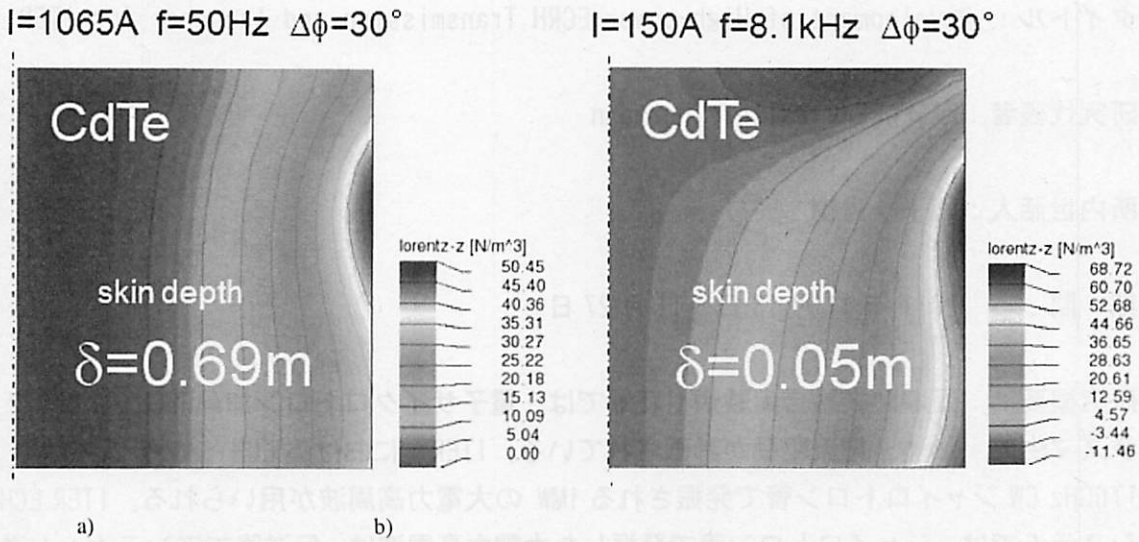

a) b)

Figure 1. Z component of Lorentz force density distribution in CdTe melts for: a) I=1065A, f=50Hz, Δϕ=30°; b) =150A, f=8.1kHz, Δϕ=30°.

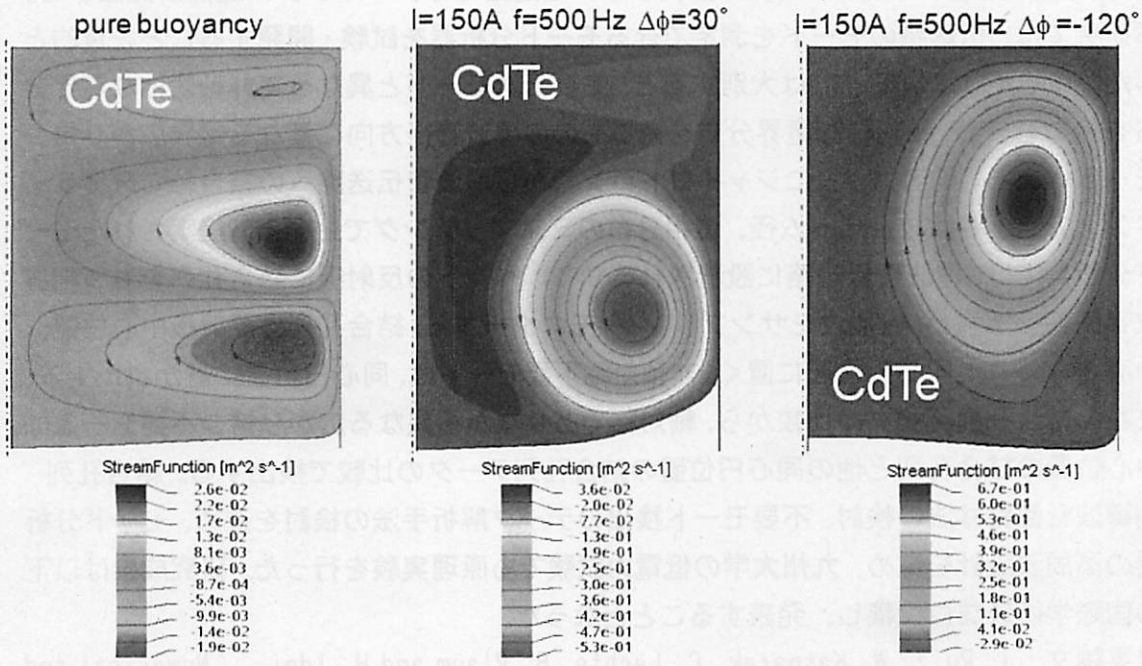

Figure 2. Stream function in CdTe melt for buoyancy driven flow (left), flow in upward directed TMF (middle) and downwards TMF (right).

国際化推進共同研究概要

No. 2

タイトル： Development of High-power ECRH Transmission and launcher for ITER

研究代表者：KASPAREK, Walter, Hermann

所内世話人：図子　秀樹

期　間：　2011年11月13日～11月27日

研究概要：　国際熱核融合実験炉(ITER)では、電子サイクロトロン加熱(ECH)によるプラズマ生成・加熱、電流駆動が計画されている。ITER　におけるECH システムでは、170GHz CW ジャイロトロン管で発振される1MW の大電力高周波が用いられる。ITER ECH システムでは、ジャイロトロン管で発振した大電力高周波は、伝送路でアンテナへと送られ、プラズマに放射される。伝送路は、オーバーサイズ導波管による要素部品で構成されており、伝送路のミスアライメント等で、主伝送モード以外の不要高次モードも励起される。励起されたモード間干渉により、伝送路でのアーキング、過熱が発生する。本研究では、伝送路のモードを測定できるモード分析器を試験・開発することを目的とした。　不要な高次モードは大別すると、主要伝送モードと異なって非軸対称な電界分布を持つモード、軸対称な電界分布を持つものの導波管径方向に異なる電界広がり持つモードがある。前者は、主にジャイロトロン管から導波管伝送路への結合軸ミスアライメントで、後者は結合ビーム径、位相分布のミスマッチングで生ずる。提案されたモード分析器では、導波管伝送路に設置される９０°ベントの反射板に結合孔列をもつ副導波管回路を準備し、伝播波をサンプリング・モニターする。結合孔列は反射板中心位置、中心から外れた同心円位置に置く。非軸対称不要モードは、同心円位置に置かれた上下、左右の結合孔列データの比較から、軸対称でありながら異なる広がり持つ不要モードは、中心位置の結合孔列と他の同心円位置の結合孔列データの比較で検出する。結合孔列・副導波管回路寸法の検討、不要モード検出のデータ解析手法の検討を進め、モード分析器の高周波設計を進め、九州大学の低電力試験でも原理実験を行った。研究成果は以下の国際学術雑誌に投稿し、発表することとなった。

成果論文：J. Ruiz, W. Kasparek, C. Lechte, B. Plaum and H. Idei, "Numerical and experimental investigation of a 5-port mitre-bend directional coupler for mode analysis in corrugated waveguides, Journal of International, Millimeter and Terahertz Waves (2012).

Report on High-power ECRH Transmission and Launcher

Applicant: Walter Kasparek

Institut für Plasmaforschung, Universität Stuttgart

The work performed under support of the Collaborative Research Program of the Research Institute for Applied Mechanics, Kyushu University, dealt with methods to characterize oversized corrugated transmission lines and launchers in high-power ECRH systems. Especially, the work performed und the collaboration aimed at the development of a high-purity HE11 mode generator and a coupler for alignment control and wrong mode detection in corrugated HE11 lines.

The International Joint Research team consisted (besides the applicant) of Hiroshi Idei (RIAM, Kyushu), Keishi Sakamoto (JAEA Naka), Takashi Shimozuma (NIFS, Toki), Richard Temkin (MIT PSFC Cambridge), Michael Shapiro (MIT PSFC Cambridge), Carsten Lechte (IPF Stuttgart), and Burkhard Plaum (IPF Stuttgart).

For the test of advanced HE11 transmission lines, mode generators with very high mode purity were developed which are compatible with the present ITER ECRH system (170 GHz, waveguide diameter 63.5 mm). Two approaches were pursued.

A resonator, which uses the HE11 field as an eigenmode, was designed and built. It consists of two mirrors, a phase-reversing mirror designed for the HE11 mode field which is defined according to the waveguide parameters on the interface plane between resonator and waveguide, and a semi-transparent plane mirror as output coupler. The excitation of the resonator was performed via a shallow phase grating and a Gaussian feed horn. Detailed measurements of amplitude and phase of the output fields, and evaluation of the efficiency and mode purity have been performed, showing that a good HE11 beam was generated. However, interference occurred with the excitation beam via the semi-transparent mirror, and thus reduced the final mode purity to a relatively low value of 94 %. As countermeasure, the feed structure is changed to a classical beam splitter, where the interference between output beam and exciting beam is avoided. This modification is underway.

The second approach was based on a synthesis of the HE11 pattern starting from the (very similar) Gaussian beam. The horn to produce this beam was calculated, and a phase-matching system based on the Kirchhoff integral on the HE11 high mode-purity generator was designed. The mirror performance has been explained well by the moment-method simulator. A very high performance with a mode purity of better than 99.8% is calculated. Design work is going on to fabricate and test this device.

A second task aimed at power monitoring, alignment control and wrong mode detection in corrugated HE11 lines. In close cooperation, 5-port coupler systems, which are integrated into a miter bend of the corrugated HE11 transmission line, where developed. Design optimizations have been performed, showing that by choosing proper positions for the coupling holes and with an appropriate signal processing, it is possible to obtain the amplitudes of 5 modes with a 5-port coupler. Especially, if the coupler structures are

optimized to detect - besides the fundamental HE11 (LP01) mode - the first higher-order symmetric LP02 mode and the first asymmetric modes LP11 (odd) and LP11 (even), then the essential basic information needed for operation of the line, namely power (from the HE11 signal), diameter matching of the gyrotron beam (from the LP02 signal), and possible misalignments (from the LP11 signals) can be obtained.
For the realization of the couplers, two prototype mitre bend mirrors with integrated couplers have been built. The first is adapted to the parameters of the ASDEX Upgrade ECRH system (140 GHz, waveguide diameter 87 mm), and is not cooled, which eases design and fabrication. This coupler could be investigated in detail during the time of the collaboration.
For experimental investigations, the dominant LP01 mode, as well as spurious modes have been excited in the waveguide, and power as well as interferometeric signals were recorded. To excite mainly the LP11 asymmetric mode, a defined tilt in the angle of incidence of the injected LP01 was introduced; the relation between tilt angle and LP11 contents was obtained from mode analysis. For detection of this mode, an interferometer between the two ports laying in the plane of the tilt was implemented.
Low-power measurements have been performed with the mitre bend installed at several locations in the waveguide run. The output signal increased monotonously with the tilt angle, independent on the position, i.e. the relative phase between LP11 and LP01; especially, the minimum of the output occurs always at the same angular position, i.e. with nominally 0 % of LP11. These results and similar findings obtained from spurious LP02 modes confirm that a 5-port mitre bend coupler is a valuable tool for mode analysis and alignment in LP01 transmission lines.
These results are also a basis for the construction of the mitre bend coupler which is designed for the parameters of the ITER transmission line (170 GHz, waveguide diameter 63.5 mm), and especially is equipped with water cooling for CW operation. The construction consists of a base plate, a body plate which contains the holes for the cooling water and the coupler waveguides, and a top plate with the hole arrays to couple a small part of the power incident to the mitre bend mirror into the coupler waveguides. The three plates to get the complete coupler mirror is jointing by brazing. This mirror is going to be ready soon, and is waiting for low-power tests at RIAM, and a possibility for high-power testing at the 170 GHz ITER test-stand at JAEA in Naka.

The results on the work on 5-port couplers were accepted for publication in a refereed journal as follows: J. Ruiz, W. Kasparek, C. Lechte, B. Plaum, and H. Idei, "Numerical and experimental investigation of a 5-port mitre-bend directional coupler for mode analysis in corrugated waveguides". Journal of Infrared, Millimeter, and Terahertz waves (2012), accepted for publication, DOI: 10.1007/s10762-012-9883-0.

To summarize, the collaborative work resulted in appreciable success in the design of components for high-power ECRH transmission lines. The parties wish to continue this collaboration to finalize the development of the pure-mode generator and the 5-port coupler mirror.

国際化推進共同研究概要

No. 3

タイトル： Development of gyro-fluid global transport code and simulation study of barrier formation.

研究代表者：DIAMOND, Patrick, Henry

所内世話人：矢木　雅敏

期　間：　2011年12月15日～12月18日

研究概要：　共同研究者の徳永晋介氏(WCI)が応用力学研究所を訪問し、プラズマ乱流に関するモデリングやシミュレーションコードの verification 等に関して議論を行った。

Development of gyro-fluid global transport code and simulation study of barrier formation

CMTFO and CASS, University of California San Diego and WCI, NFRI, P. H. Diamond

Objectives

Realization of advanced tokamak operation in ITER and future reactors requires operating plasma in steady state enhanced confinement regime. It is expected that the anomalous transport due to plasma turbulence is reduced in such an improved confinement regime. Experiments and numerical simulations have often shown that there exists nonlocal transport governed by meso-scale dynamics. A natural consequence of the existence of nonlocal transport would be the possible breaking of the local mixing length-type gyroBohm transport scaling, in particular when turbulence spreading or avalanches pertains. Both improved confinement and nonlocal transport are crucial subjects, however have not fully elucidated. The objective of this study is to investigate characteristics and impacts of avalanching heat transport in steady state enhanced confinement regime.

Method

Detailed analysis of fully flux-driven steady state with improved confinement region around q-minimum position of reversed magnetic shear profile obtained from longtime global gyrofluid simulation was performed. A gyrofluid model based on the TRB code [X. Garbet, et al., Phys. Plasmas **8**, 2793 (2001), S. S. Kim, et al., Nucl. Fusion **51**, 073021 (2011)] was employed. Following analyses were carried out to investigate the avalanching transport property and its dependence on degree of turbulence suppression (Nusselt number).

(1) Analysis of flux-driven steady state with enhanced confinement regime
(2) Probability distribution function (PDF) of heat flux
(3) Power spectrum density (PSD) of heat flux and frequency resolved heat flux
(4) Spatial correlation of heat flux and crosscorrelation between heat flux and ExB shearing rate
(5) Temporal autocorrelation and Hurst exponent of heat flux
(6) Quiet time distribution of heat avalanche

Results

Flux-driven steady state enhanced confinement regime around q-minimum position was observed. Apparent change of tendency of relationship between turbulent flux and gradient (i.e. χ^{turb}) in this improved confinement layer depending on the amplitude of heat source was found. It suggests drastic qualitative difference of dominant transport mechanism between weak and strong barrier cases. We calculated time-averaged Nusselt number to refer the weak and strong barrier cases as

High-Nu (Nu~11) and Low-Nu (Nu~3) cases respectively. The heat flux PDF in these improved confinement regime shows prominent "fat tail" and it yields significant deviation from the Gaussian distribution. The kurtosis in low-Nu case reaches up to ~ 9 (3 for Gaussian). Such tail should correspond to the large-scale transport event, i.e. heat avalanche. Cumulative PDF shows that the tails are responsible to ~20% and ~50% of total turbulent heat flux in high- and low-Nu cases, respectively. Considerable impact of avalanching transport in improved confinement regime was clearly shown. PSD of heat flux indicates marked difference between two cases. In high-Nu case, PSD shows distinct peaks (f ~$1\times10^{-3}c_s/a$), much lower than drift frequency. It indicates salient quasi-periodic (QP) pulsatory transport dominates the system. On the other hand, in low-Nu case, broad 1/f frequency band appears. Such PSD implies presence of longtime correlation. Contribution from these peaks or bands to total flux estimated from frequency resolved heat flux agreed to from PDF. For QP pulse, 2-point correlation analysis revealed strong spatial correlation covering whole radial extent of the system. QP heat pulse indicates clear crosscorrelation to ExB shearing rate ($\gamma_{E\times B}$). We confirmed that collisional damping rate of zonal flow determines the period of QP. Then it could be interpreted by mechanism shown by Kim and Diamond [E. J. Kim and P. H. Diamond, Phys. Rev. Lett. **90**, 185006 (2003)]. In contrast, 1/f avalanche hardly shows correlation to $\gamma_{E\times B}$. 2-point correlation showed clear shrink of correlation length of heat flux in low-Nu case. Autocorrelation of heat flux obeys power law. Then existence of long-time correlation of heat flux in improved confinement regime was confirmed. Steady state barrier region can be not completely steady. Importance of avalanching transport and its spatio-temporal non-locality was clearly shown.

Report

[1] S. Tokunaga, Hogun Jhang, S. S. Kim, P. H. Diamond, "Avalanching heat transport in steady state internal transport barriers with reversed magnetic shear", 1st Asia Pacific Transport Working Group International Conference, B-P9, Toki, Japan, June 2011.

[2] S. Tokunaga, Hogun Jhang, S. S. Kim, P. H. Diamond, "Analysis of avalanches originated in q-minimum region", 2nd US-Japan JIFT workshop on "Hierarchical Self-Organization of Turbulence and flows in Plasmas, Oceans and Atmospheres", 23, Kyoto, Japan, October 2011.

[3] S. Tokunaga, Hogun Jhang, S. S. Kim, P. H. Diamond, "Avalanching heat transport in steady state ion internal transport barriers with reversed magnetic shear", to be submitted to Plasma Phys. Control. Fusion.

Participants

Representative person: P. H. Diamond (CMTFO and CASS, UCSD and WCI, NFRI)

Advisor: M. Yagi (RIAM, Kyushu University and JAEA)

Co-worker: S. Tokunaga (WCI, NFRI)

国際化推進共同研究概要

No. 4

タイトル：Comparative and joint study of steady state operation(SSO) of high temperature plasmas and related plasma wall interaction(PWI) on QUEST and EAST.

研究代表者： Gao Xiang 教授・Liu Haiqing 氏 Institute of Plasma Physics,Chinese Academy of Sciences

所内世話人：花田 和明

来訪期間 ： 2012 年 1 月 18 日 ～ 2012 年 1 月 31 日

概要： QUEST の ECR プラズマ中の Blob 現象のデータ取得を行った。実験準備を含めて3日間の実験の一部の放電をこの共同研究のために実施した。観測は、既設の高速カメラと静電プローブを併用し、段階的に磁力線の結合長を変えることで Blob の伝播速度がどのように変化するかを調べる実験を行なった。予定していたデータはすべて取得し、現在解析中。

成果（論文）

R. Ogata, K. Hanada, N. Nishino, H. Q. Liu, H. Zushi, M. Ishiguro, T. Ikeda, K. Nakamura, A. Fujisawa, H. Idei, M. Hasegawa, S. Kawasaki, H. Nakashima,
A. Higashijima, and QUEST group:
「 Investigations of the Radial Propagation of Blob-like structure in a Non-Confined ECRH plasma on QUEST」 Physics of Plasmas 18.092306

発表

Experimental observation and Statitstical Analysis of Blob-like structures in QUEST APFA2011(8th General Scientific Assembly of the Asia Plasma and Fusion Association)Nov 1st to 4th Guilin,CHINA

特記事項

AFFAでのこの共同研究に関する発表が young scientist award（最優秀賞）に選ばれた。

(様式 11・拠点)

RESEARCH REPORT

Date Jan. 31, 2011

Visiting scientists: (name) Xiang Gao

(position) Professor

(university / institute) Institute of Plasma Physics,
Chinese Academy of Sciences

(name) Haiqing Liu

(position) Assistant Professor

(university / institute) Institute of Plasma Physics,
Chinese Academy of Sciences

Host scientist: (name) Kazuaki Hanada

(position) Professor

(university / institute) Kyushu University

Research period: (from) Jan. 18, 2012 (to) Jan.31, 2012

Research subject: **Study of Blob-like Structures in QUEST**

Introduction

Recently experimental and theoretical works suggested importance of 'blob' type fluctuation in edge plasma, usually observed by some probes or cameras in many devices and configurations. These structures contain excess density and temperature as compared with the background plasma and possibly lead to serious wall erosion, impurity production, heat and particle load, and particle recycling that may become critical for ITER. Recently measurements reveal parallel currents associated with blob-like structures or filaments during ELMs, which result in large net currents to divertor plates. The importance of parallel currents on blob propagation could be inferred by comparing experimental blob speed-versus-size scaling with theory predictions.

Firstly, according to the model of radial propagation velocities, blobs basically propagated to the low field side riding on $E \times B$ drift, where E and B show electric field to poloidal direction and toroidal magnetic field, respectively. The electric field can be originally formed by self-induced charge separation due to grad-B and curvature drifts and keeps a certain value via current paths through sheathes at attached region of metallic walls. The existence of two regimes for blob propagation, when sheath losses become dominant,

$$V_{she} = \left(\frac{\rho_s}{a}\right)^2 \frac{L_c}{R} C_s \frac{\delta n}{n} \cdots ①$$

;

when the divergence of the ion polarization current become dominant,

$$V_{pol} = \sqrt{\frac{2a}{R}} C_s \frac{\delta n}{n} \cdots ②$$

,

where V is radial velocities of blob, a is blob size, L_c is the connection length, C_s is the plasma sound speed, R is the major radius, ρ_s is the ion gyro-radius, $\delta n/n$ describes the slowing down by limited background density, as shown in Figure 1. In which parallel currents to the sheath, respectively, do or do not efficiently damp the grad-B and curvature induced polarization of the blob. Connection length is important due the existence of sheath connection, in which the sheath do significantly damp charge separation and thus blob radial velocity. Secondly, according to the recent results in QUEST, when the pitch of a

blob-like structure is shortened, the return current may flow between the pitch. However the threshold is unclear now. To change the pitch angle (B_z scan, B_t scan) and thus connection length for investigating the blob speed-versus-size scaling and the regime of blob propagating are done in this experiment. Thirdly, the blobs were also was observed in HT-7 and EAST tokamak. To compare the basic parameters (V_b, S_b, statistical information) with different devices and discharge conditions is important for finding the basic principle of blobs. So this experiment will contribute to blob comparison study in QUEST, HT-7 and EAST. These motivate the development of experiment of blob and dedicated physics study here.

Experimental setup

QUEST is a medium sized spherical tokamak, which has advantage of improved high beta stability compared to conventional tokamaks and charged with a mission to study issues related to steady-state operation. And it has a major radius of R = 0.68 m, minor radius of a = 0.40 m, diameters of the center stack and the outer wall of ~ 0.2 m and ~ 1.4 m, respectively and flat divertor plates at the vertical distance from the midplane, $Z = \pm$ 1 m. Microwave heating power of 8.2 GHz up to 400 kW and 2.45 GHz up to 50 kW was prepared for plasma heating.

In this experiment, hydrogen plasma were initiated by using electron cyclotron resonance heating (ECRH) at 2.45 GHz in open configurations. Plasma was located around fundamental ECR layer and had no confined region. The injected microwave power for ECR heating was about ~ 10 kW. A scanned vertical magnetic field of 0~19 mT is superimposed on a scanned toroidal field of 35-65 mT to form helical field lines. Typical plasma parameters in the edge of plasma are $n_e \sim 10^{16}$–10^{17} m^{-3} and $T_e \sim$ 1–10 eV, with peak values about twice as high. Other relevant parameters are $c_s \sim 10-34 km/s$, $\rho_s \equiv c_s / \omega_{ci} \sim 3-9 mm$ and $\lambda_{mfp}^{ei} \square \lambda_{mfp}^{en} = o(1)m$, in this regime the

dominant collision channel are Coulomb collisions. The plasma beta is as low as $\beta \sim 10^{-4}$. A combination of a fast camera (FC), a movable Langmuir probe(LP) and divertor probes (DP) were used, as shown in Figure2. The LP composed of six tungsten -pins are set at in radial direction of R = 100 cm. The six pins' diameter and length are 1 mm^{Φ} × 1 mm^{L}, separated by 5 mm in toroidal and vertical directions. It allows the simultaneous measurement of the ion saturation current, I_s, floating potential, V_f and positive bias with a high temporal resolution (1MHz). The electron temperature, T_e, and density, n_e, are measured by using the triple-probe principle. Seven pins of the DP are used to measure I_s (pins 1,7,13,19,25,31) and V_f (pin 30)with a high temporal resolution (1MHz). DP pins' diameter and length are 3 mm^{Φ} × 2 mm^{L}. The pin1 has a 83mm distance to the central stack, and every two pins distance in radial direction is 15mm. Density and plasma potential fluctuations can be estimable from I_s and V_f, respectively, by neglecting electron temperature fluctuations effects.

The FX-K5 fast camera was typically set at 20000 FPS with 288 × 240 pixels each frame, each pixel is about 1.5 cm in size. Its viewing area can cover the plasma space where the Langmuir probe can be manipulated in the radial direction, as shown in Figure 3.

Primary results

One of main experiments is PF coil current scan. The toroidal field ,B_t, was set at 40 mT, the PF coil current was scan from 0 to 1.5 kA and thus the vertical field, B_z, scan from 0 to 19 mA. When the B_z/B_t increasing, the fast camera imaging show the blob-like structures change to more strong and clear structures, as shown in figure 4. There is an abundance of intermittent large amplitude bursts in time series in singal of LP. These bursts are identified

with blob-like structures. as shown in Figure 5. The intensity and frequency of bursts events are vary with the B_z and then the connection length. The probability distribution function (PDF) of density fluctuations (I_s) are used to investigate the shape feature of blob-like structure and the deviation degree from the Gaussian distribution, as shown in Figure 6. In step 1, I_{pf26}=0.1kA, the PDF is near to Gaussion distribution, and the blob-like structure not so strong. The PDF was changed into stronger non-Gaussion distribution with bigger PF coil current from 0.2kA to 1.5kA. That is mean that the bursts in the density fluctuation signals have more asymmetry structures.

The other of main experiments is TF coil scan. The TF coil current was scanned from 7kA to 13kA step by step in three shots. For keeping the pitch angle in same value, the PF coil current was scaned from 0.7kA to 1.3kA, respectively. The pitch angle and thus connection length keep close value during this scan. From the fast camera imaging, the blob-like structures keep in similar sharp and field aligned filament structures, as shown in Figure 7. The PDF of density fluctuation signals from the Divertor probe (I_s31:R=808.75mm) was shown in Figure 8, when the TF coil current was scanned from 11kA to 13kA, the 1st ECR layer was shifted to outside from R=400mm to R=470mm. The PDF signal was change from strong non-Gaussion distribution into weak non-Gaussion distribution. It is indicate that the blob-like structure near to the main plasma has weak blob characteristic. When it propagating in radial direction, blob-like structures show strong sharp and clear field aligned filament structure due to the charge separation by grad-B. The PDF of density fluctuation signals from the Langmuir probe in mid-plane (I_s1:R=1000 mm) was shown in

Figure 9, similar strong non-Gaussion distribution was found. It is indicate that there is similarity structure of blob in far SOL-like area.

Conclusion

The PF scan (to change the pitch angle and connection length) and TF scan(to change the ECR layer position and thus main plasma position) experiments was done to investigate blob-like structures' characteristic in QUEST. Fast camera, Langmuir probe in mid-plane and divertor probes are used to observed the blobs. Experiment in plan was obtained successfully. More detailed analysis will be done soon. These results will be combined with previous experimental results in QUEST and then compared with blob results in HT-7 and EAST tokamak.

Acknowledgement and comments:

Work supported by the international joint research at the Joint Usage of Research Centers for Applied Mechanics for 2011. We would like to thank our host, Professor K. Hanada, who helps a lot during my staying at QUEST and very appreciate the useful discussion and comments. Mr. Ishiguro, Mr. Takahashi and Mr. Yamada also gave us so many help on our stay in Kyushu University. My thanks are also expressed to them and the QUEST group.

It is a good chance for us to join in the experimental study in the QUEST. We hope that the international joint research at the Joint Usage of Research Centers for Applied Mechanics could continue to enhance China-Japan cooperation on fusion plasma research in the future.

Figure captions:

Figure 1 grad-B and curvature driven plasma polarization and associated E × B drift result in outward motion of blobs in tokamak far scrape off layer. Schematic of current loops arising from the charge separation current. Two regimes for blob propagation, (1) Sheath losses become dominant; (2)Divergence of the ion polarization current become dominant.

Figure 2 (a) A schematic view of a first wall; a typical magnetic flux surface; an ECRH plasma located in the region of the 1st ECR resonance layer (vertical red line, R = 30 cm) and 2nd ECR resonance layer (vertical green line, R = 60 cm); propagating blob-like structures; and measureable radial position of the probe system in a poloidal cross-section of QUEST, the photo of probe head was shown in (a1); (b) A sketch of 3-D 'blob-like structures' in QUEST, the divertor probe was enlarged and shown in (b1).

Figure 3 (a) A photo of fx-K5 fast camera; (b) A topview of experimental setup. The positions of fast camera, Langmuir probe in midplane and divertor probe are shown; (c) A fast camera picture of blob-like structure was shown.

Figure 4 Fast camera images with five steps of PF coil current scan, probe head location was marked with red circles (shot No.:17952).

Figure 5 I_s and V_f signal in Langmuir probe in midplane during PF coil current scan (shot No.:17952).

Figure 6 Probability distribution functions of the I_s (I_s1 in LP) fluctuations with five step PF coil currents(i:0.1kA, ii:0.2kA, iii:0.4kA, iv: 0.8kA, v:1.5kA) (shot No.:17952).

Figure 7 Fast camera images with three steps of TF coil current scan, TF coil current, i: 11kA, ii: 12kA, iii: 13kA, PF coil current, 1.1kA, 1.2kA,1.3kA, respectively(shot No.:17959).

Figure 8 Probability distribution functions of the I_s (I_s31 in DP) fluctuations with three steps TF coil currents(i:11kA, ii:12kA, iii:13kA) (shot No.:17959).

Figure 9 Probability distribution functions of the I_s (I_s1 in LP) fluctuations with three steps TF coil currents(i:11kA, ii:12kA, iii:13kA) (shot No.:17959).

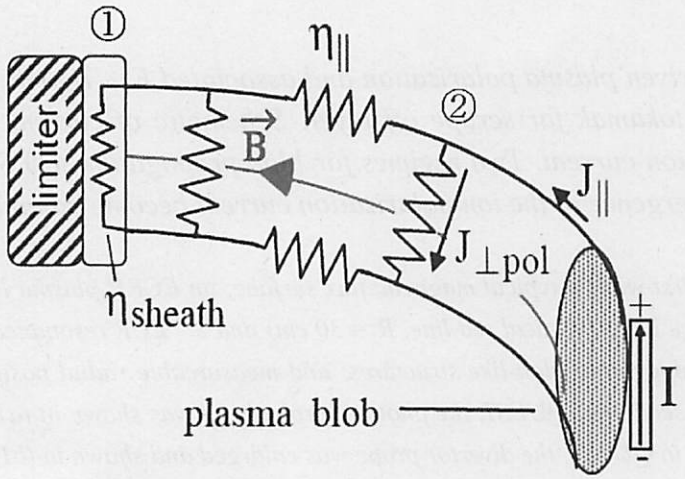

Figure 1 grad-B and curvature driven plasma polarization and associated E × B drift result in outward motion of blobs in tokamak far scrape off layer. Schematic of current loops arising from the charge separation current. Two regimes for blob propagation, (1) Sheath losses become dominant; (2)Divergence of the ion polarization current become dominant.

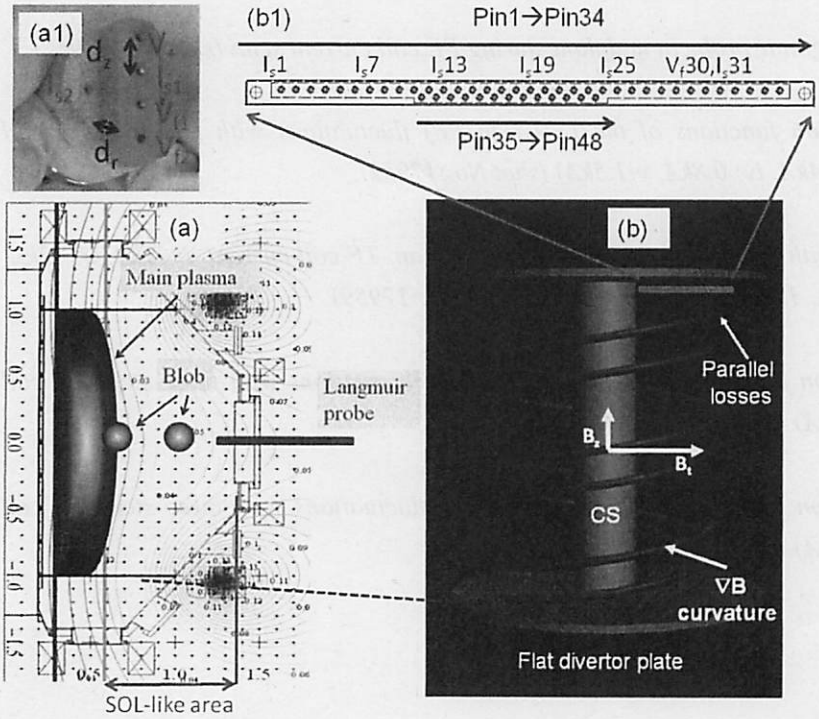

Figure 2 (a) A schematic view of a first wall; a typical magnetic flux surface; an ECRH plasma located in the region of the 1st ECR resonance layer (vertical red line, R = 30 cm) and 2nd ECR resonance layer (vertical green line, R = 60 cm); propagating blob-like structures; and measureable radial position of the probe system in a poloidal cross-section of QUEST, the photo of probe head was shown in (a1); (b) A sketch of 3-D 'blob-like structures' in QUEST, the divertor probe was enlarged and shown in (b1).

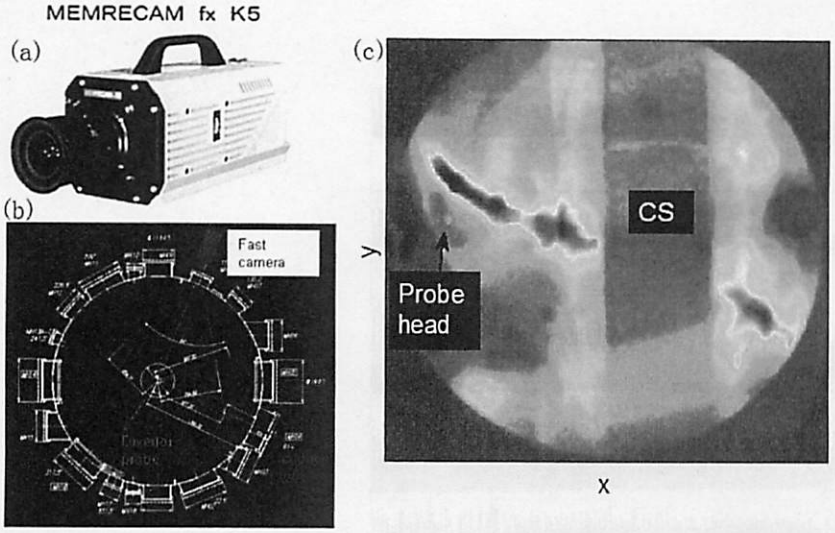

Figure 3 (a) A photo of fx-K5 fast camera; (b) A topview of experimental setup. The positions of fast camera, Langmuir probe in midplane and divertor probe are shown; (c) A fast camera picture of blob-like structure was shown.

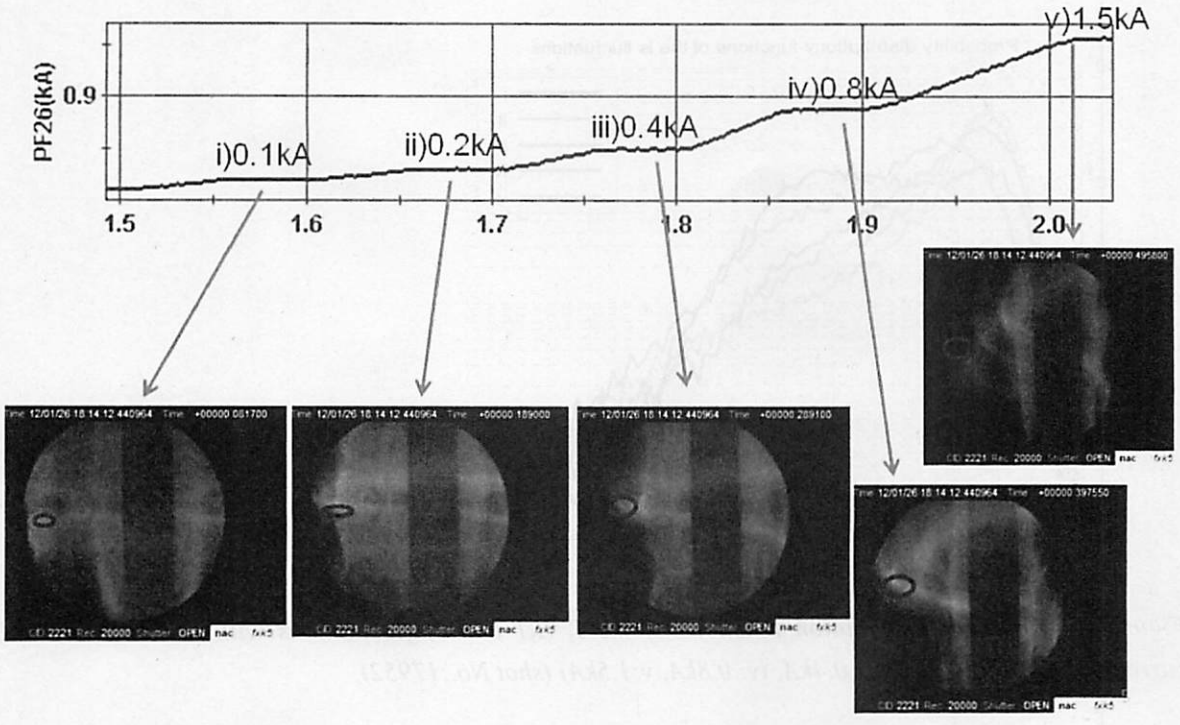

Figure 4 Fast camera images with five steps of PF coil current scan, probe head location was marked with red circles (shot No.:17952).

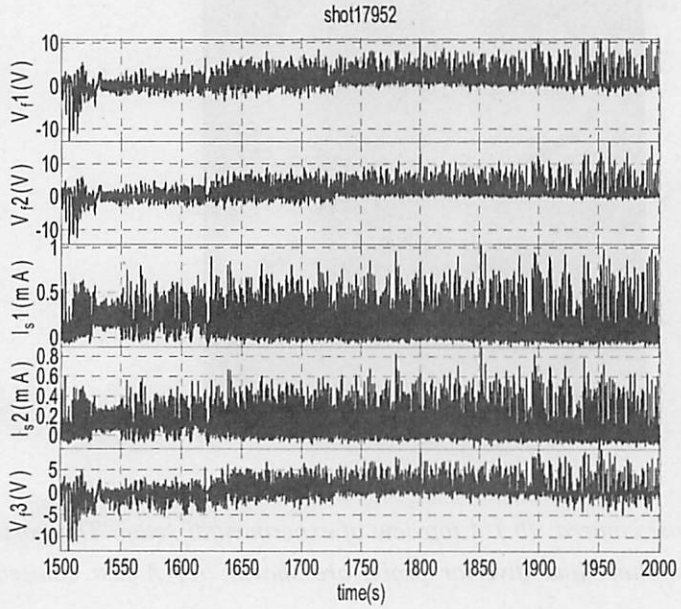

Figure 5 I_s and V_f signal in Langmuir probe in midplane during PF coil current scan (shot No.:17952).

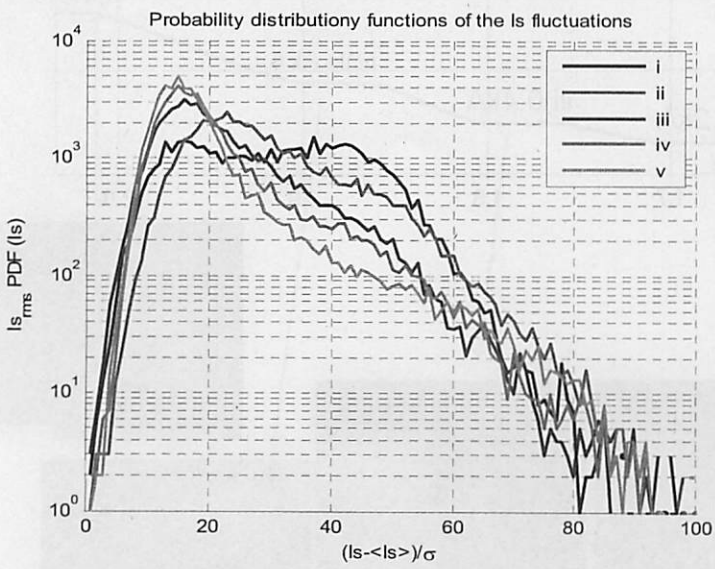

Figure 6 Probability distribution functions of the I_s (I_s1 in LP) fluctuations with five step PF coil currents(i:0.1kA, ii:0.2kA, iii:0.4kA, iv: 0.8kA, v:1.5kA) (shot No.:17952).

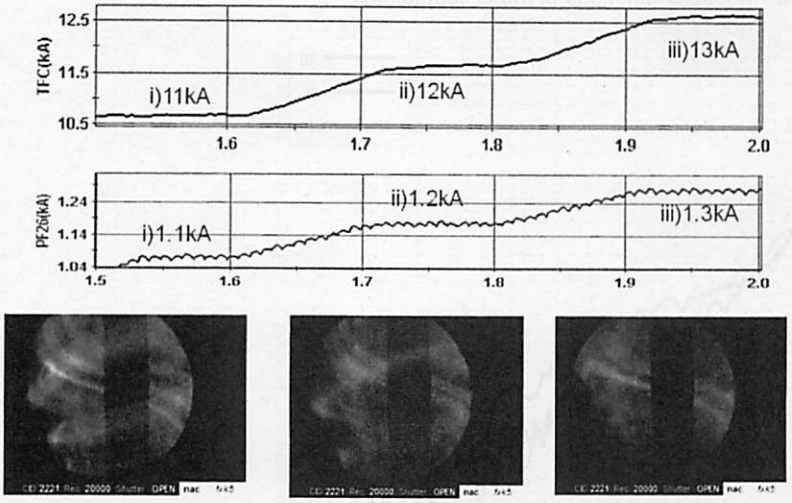

Figure 7 Fast camera images with three steps of TF coil current scan, TF coil current, i: 11kA, ii: 12kA, iii: 13kA, PF coil current, 1.1kA, 1.2kA,1.3kA, respectively(shot No.:17959).

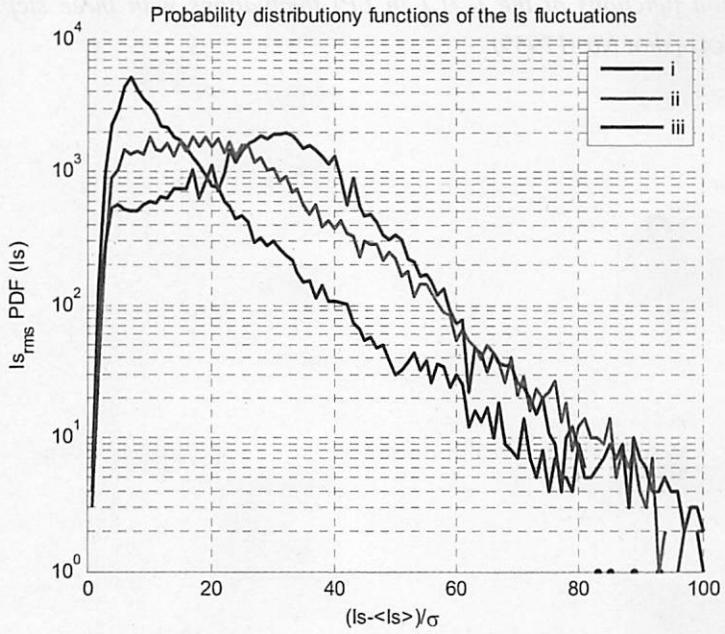

Figure 8 Probability distribution functions of the I_s (I_s31 in DP) fluctuations with three steps TF coil currents(i:11kA, ii:12kA, iii:13kA) (shot No.:17959).

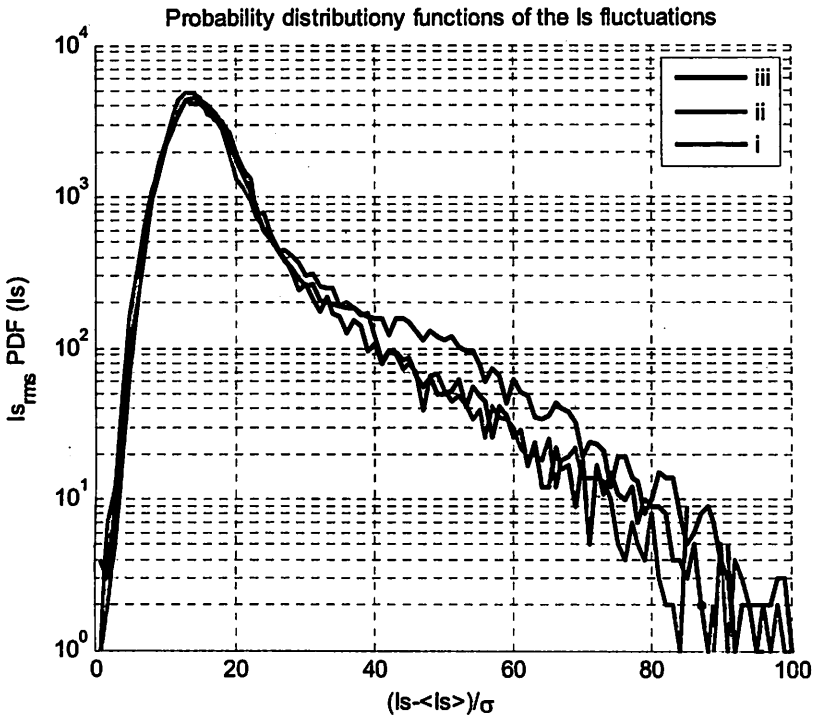

Figure 9 Probability distribution functions of the I_s (I_s1 in LP) fluctuations with three steps TF coil currents(i:11kA, ii:12kA, iii:13kA) (shot No.:17959).

(Signature) _____

(Name in print) Xiang Gao, Haiqing Liu

国際化推進共同研究概要

No. 5

タイトル;Develop and improve EFIT code of the plasma equilibrium reconstruction for SSO operation and advanced physical study on QUEST

研究代表者: Qian jinping 氏

所内世話人: 花田 和明

来訪期間: 平成 23 年 10 月 31 日～11 月 16 日

概要:QUESTで使用している平衡コードEFITをダイバータ配位に対応できるように改造を行なった。また、新規で設置した計測用の磁気コイルの校正を行い、EFIT 内のデータとして使用で きるように EFIT を変更した。また、QUEST側で整備した2次元の軟エックス線分布をEFIT の平衡計算に適応できるようにコードの改造を行った。計算された平衡配位は以下の論文の一部の図面として活用されている。

成果(印刷論文)

K. Hanada, H. Zushi, H. Idei, K. Nakamura, M. Ishiguro, S. Tashima, E. I. Ka linnikova, M. Sakamoto, M. Hasegawa, A. Fujisawa, A. Higashijima, S. Kawasaki, H. Nakashima, H. Liu, O. Mitarai, T. Maekawa, A. Fukuyama, Y. Takase and J. Qian: Non-Inductive Start up of QUEST Plasma by RF Power, Plasma Science and Technology, Vol. 13, No.3, 307-311 (2011)

Kazuaki Hanada,Hideki Zushi,Hiroshi Idei,Kazuo Nakamura,Masaki Ishiguro,Saya Tashima,Evgeniya Kalinnikova,Mizuki Sakamoto,Makoto Hasegawa,Akihide Fujisawa,Konosuke Sato,Naoaki Yoshida,Hideo Watanabe,Kazutoshi Tokunaga,Yoshihiko Nagashima,Aki Higashijima,Shoji Kawasaki,Hisatoshi Nakashima,Haiqing Liu,Osamu Mitarai,Takashi Maekawa,Atsushi Fukuyama,Yuichi Takase,Jinping Qian
QUEST experiments towards steady state operation of spherical tokamaks
IEEJ to be published

RESEARCH REPORT

Date Nov. 15 2011

Visiting scientist: (name) Jinping Qian

(position) Assistant Professor

(university / institute) Institute of Plasma Physics,
Chinese Academy of Science

Host scientist: (name) K. Hanada

(position) Professor

(university / institute) Kyushu University

Research period: (from) Oct. 31, 2011 (to) Nov.16, 2011

Research subject:

Magnetic sensor calibration and Equilibrium reconstruction on QUEST

The rapid and accurate determination of the equilibrium configuration is important for the real-time plasma control and off-line analysis of physical experiments. Measurements of the external magnetic field and flux are the key data for the reconstruction of plasma boundary. The uncertainties or standard errors of magnetic data used in plasma equilibrium reconstruction are relative to the fitting weight. Therefore, the uncertainty analysis of these magnetic data is important and indispensable.

The Quest (Q –shu University Experiment with Steady State Spherical Tokamak) project focuses on the steady state operation. The magnetic measurements consist of 67 flux loops, 1 Rogowski loop and the new mounted five magnetic probes (see figure 1). All poloidal field (PF) coils are set in 5 groups {PF4-(1, 2 and 3) + CCU + CCL, PF35-12, PF26, PF17 and HCUL} and equipped by 5 power supplies. Note that HCU and HCL are in anti-parallel connection to control the vertical displacement.

Benchmarking and test were performed to estimate the overall uncertainties of the magnetic data with the 13 vacuum shots. To ensure no vessel current induced in the magnetic measurements, the currents in the PF coils are held at their flat-top values for a period much longer than the resistive skin time of the vessel. The wave forms of the vacuum shot are shown in figure 2. Comparisons of the magnetic data against those predicted are presented in figure 3. As is shown, most signals of measured match those predicted well. Moreover, each PF coil current were fitted by the flux loop mounted on the high field. The final uncertainties of the magnetic measurements are shown in figures 4-6. The errors of PF coil current, flux loop and magnetic data are in levels of 20A, 5mWb and 10-15Gauss, separately.

Two examples using external magnetic data are presented to illustrate equilibrium reconstructions in quest. The reconstruction is made using the polynomial representation for P' and FF'. A 65×65 (65 grid points in the R and Z direction, respectively) version of

EFIT is used with a relative equilibrium convergence error (10−3). The reconstructed plasma shape, global parameters are shown in Fig. 7

For the understanding of MHD stability and physical experiments of tokamak, it is essential to obtain information on the internal plasma current and safety-factor q profiles. A comprehensive method to self consistently reconstruct the equilibrium current and q profiles with magnetic and internal iso-flux constraints are tested in the equilibrium fitting code EFIT. The iso-flux constraint can be expressed as

$$\sum_i \left[G^+_{C_i}\left(\bar{r}^+_{si},\bar{r}_{ej}\right) - G^-_{C_i}\left(\bar{r}^-_{si},\bar{r}_{ej}\right)\right] I_{ej} + \int_{\Omega^m} dR'\,dZ'$$

$$\times \left[G^+_{C_i}\left(\bar{r}^+_{si},\bar{r}'\right) - G^-_{C_i}\left(\bar{r}^-_{si},\bar{r}'\right)\right] J_\phi\left[R',\psi^m\left(\bar{r}',\bar{\alpha}^{m+1}\right)\right] = 0 \quad .$$

Here, + and – denote the i^{th} pair of data points.

A comparison of reconstructed current density J profile and plasma boundary with those from magnetic data equilibrium is shown in figure 8. This can be an alternative method to provide the useful current or q profile information for those devices without MSE diagnostic system.

Acknowledgement:

It's my honor to work with a number of excellent people on QUEST device. I would like to thank my host, Professor K. Hanada, who helps a lot. The financial support for this project by Kyushu University is gratefully acknowledged.

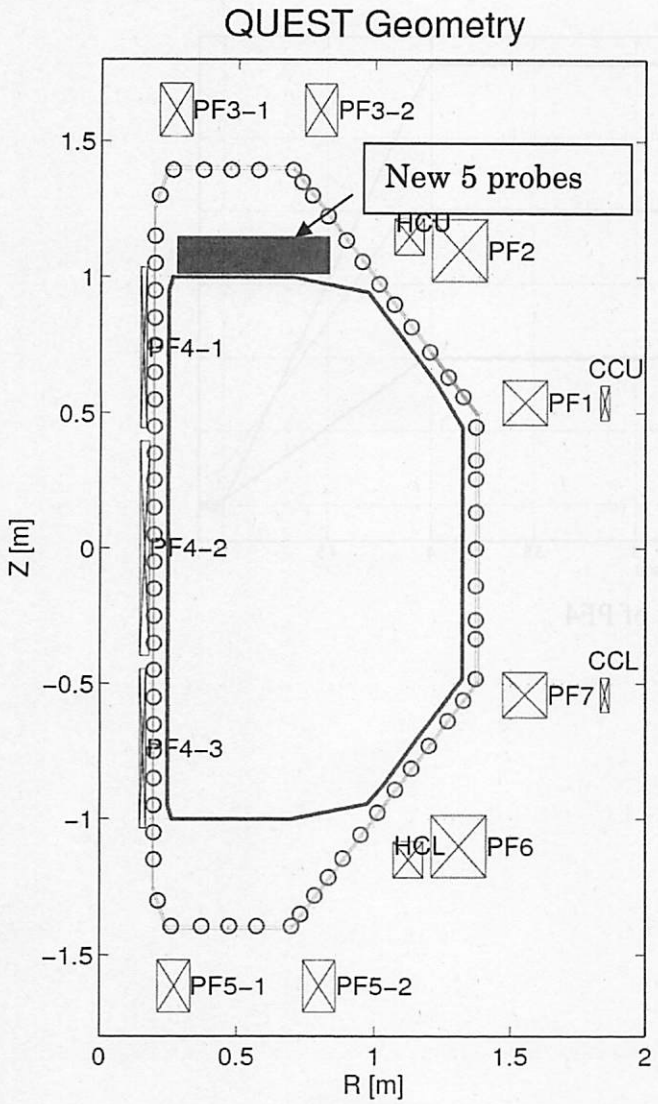

Figure 1 Quest device cross-section with flux loops (open circle) and new mounted magnetic probes

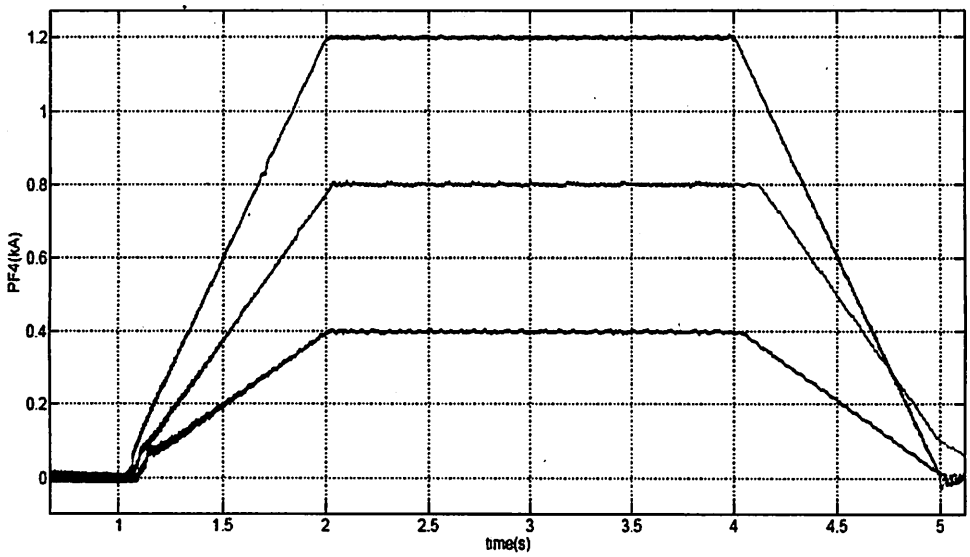

Figure 2 wave forms of the vacuum shot of PF4

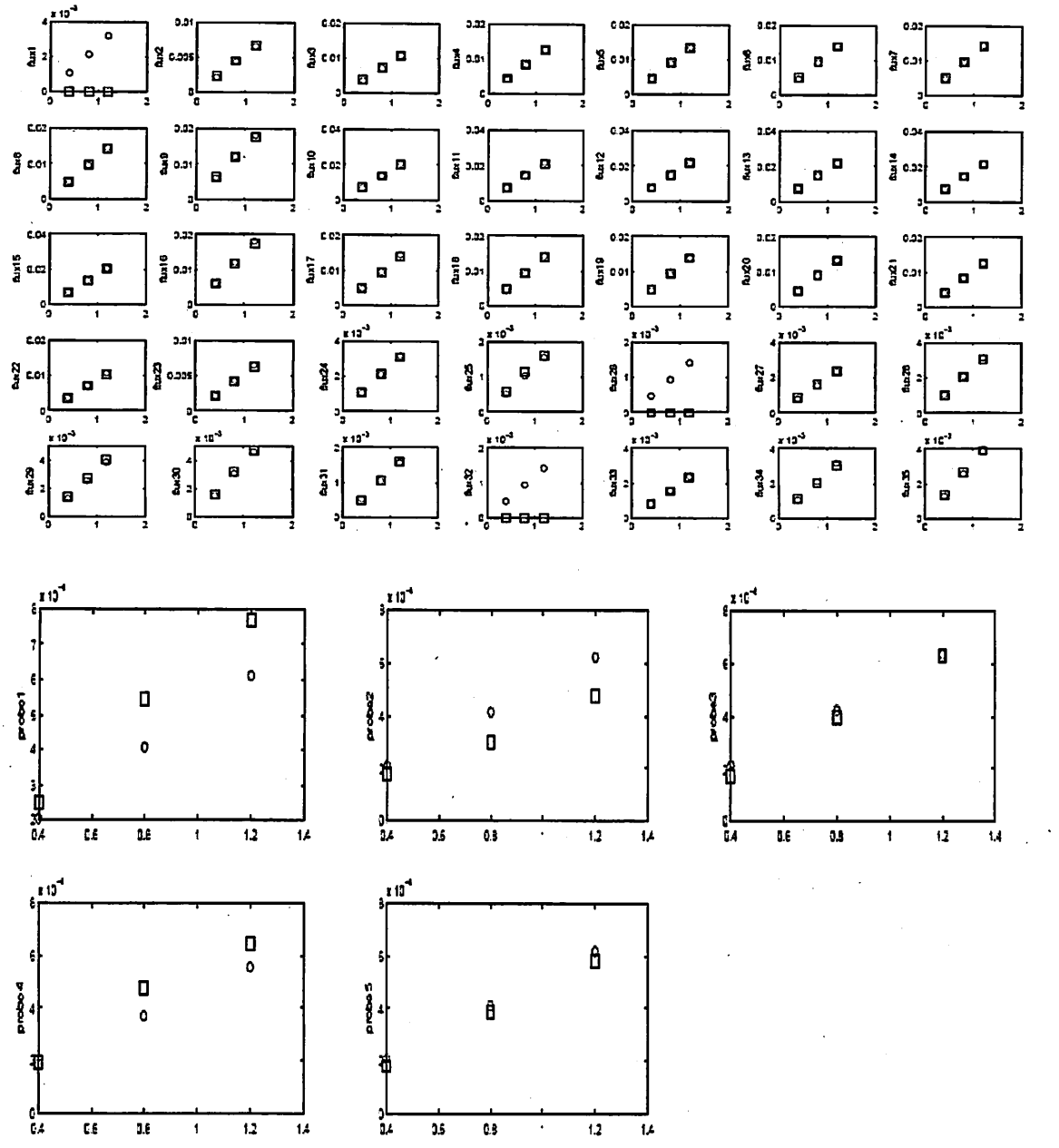

Figure 3 PF4 vacuum shot benchmarking at 3.5s (open circle: calculated and open square: measured). The horizontal axis is related to PF coil current in kA unit.

PF4 (KA)	Pf4 fitting	pf35	pf35	pf26	pf26	Pf17	pf17	HCUL	HCUL
0.4002	0.4125	1.002	1.035	0.4	0.4076	0.9981	1.009	0.0998	0.097
0.7999	0.8079	2.505	2.564	0.8001	0.8127	1.9957	2.0326		
1.2	1.1919	4.047	4.047	1.2	1.2341	2.9953	3.0435		

Figure 4 All PF coil measurements against those fitted by flux mounted on the field

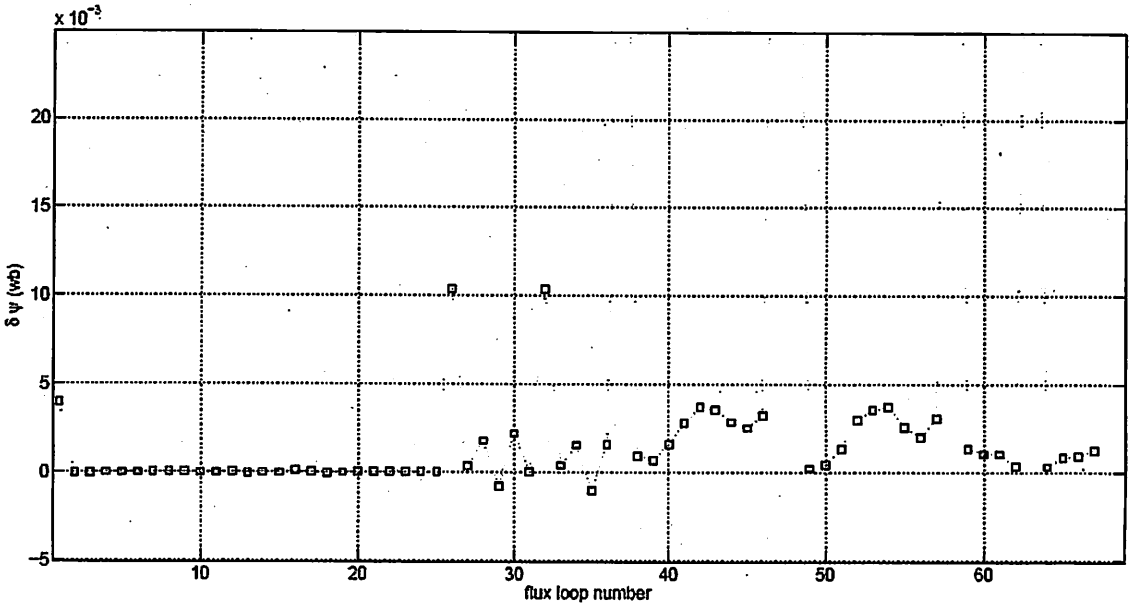

Figure 5 uncertainty of the flux loop

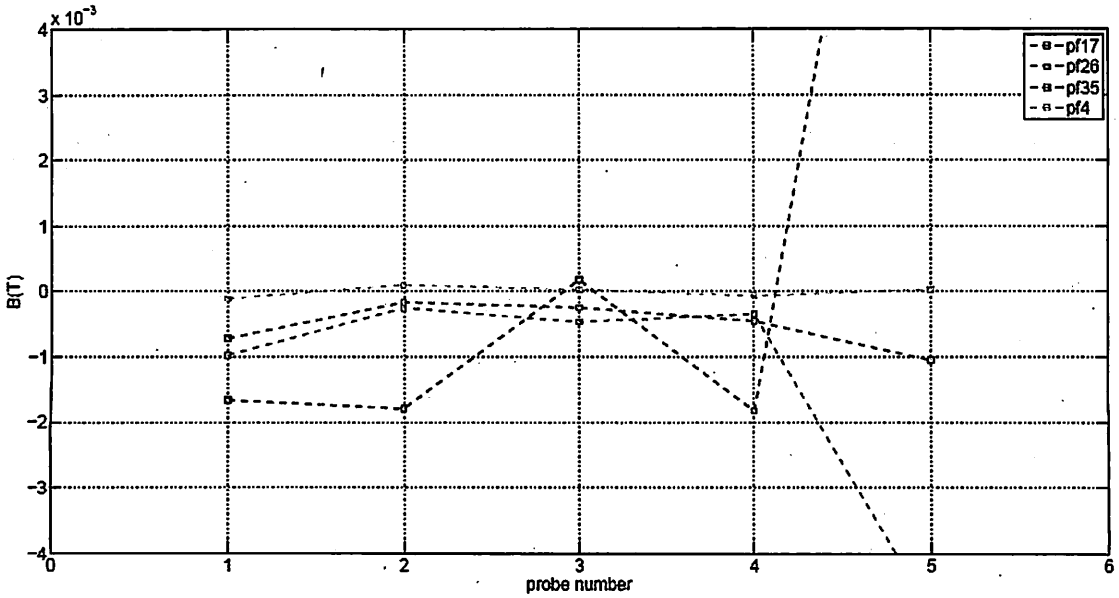

Figure 6 magnetic probes uncertainty

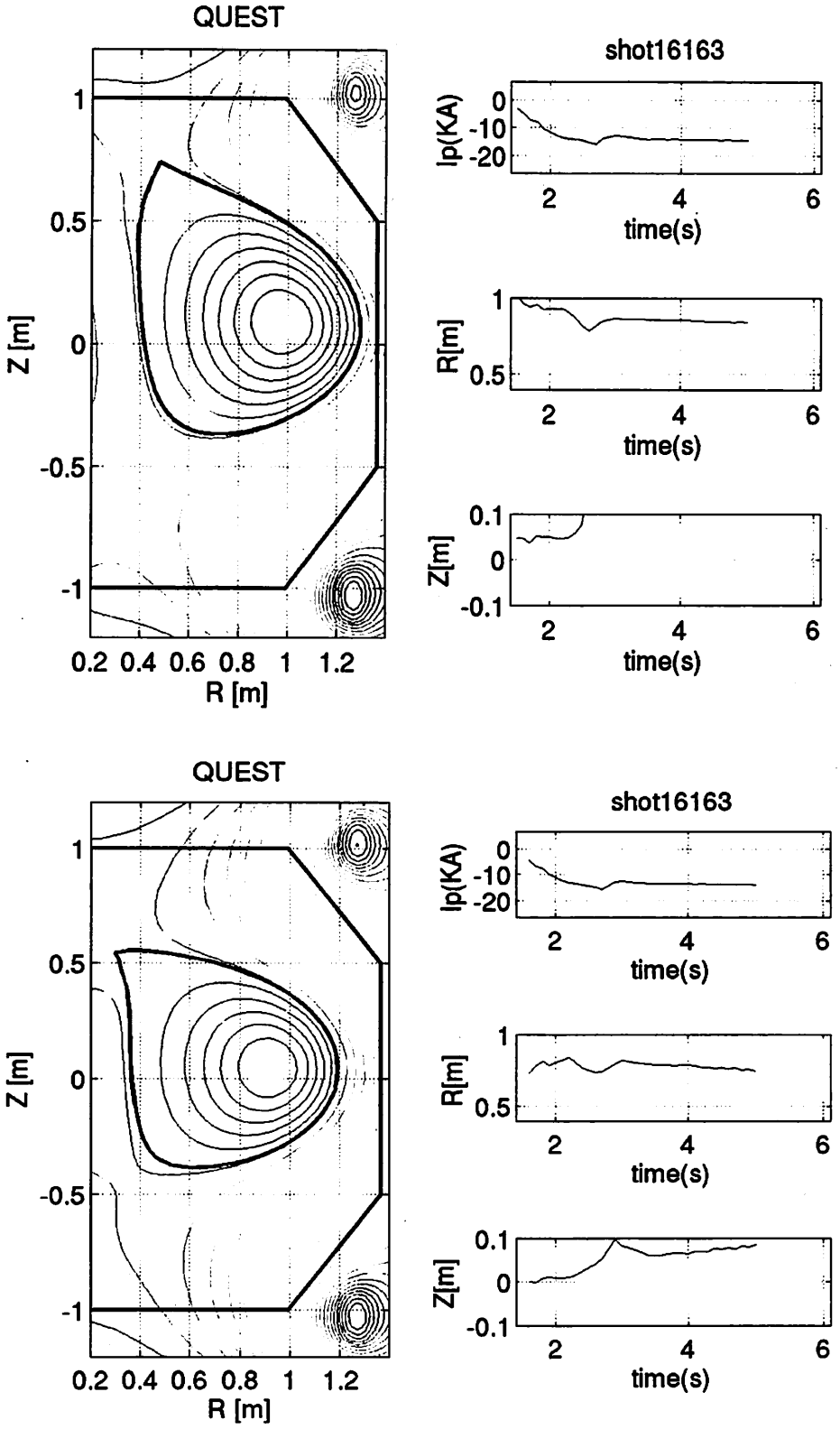

Figure 7 equilibrium reconstruction with the magnetic data (top: flux loop +magnetic probe; bottom: flux data only)

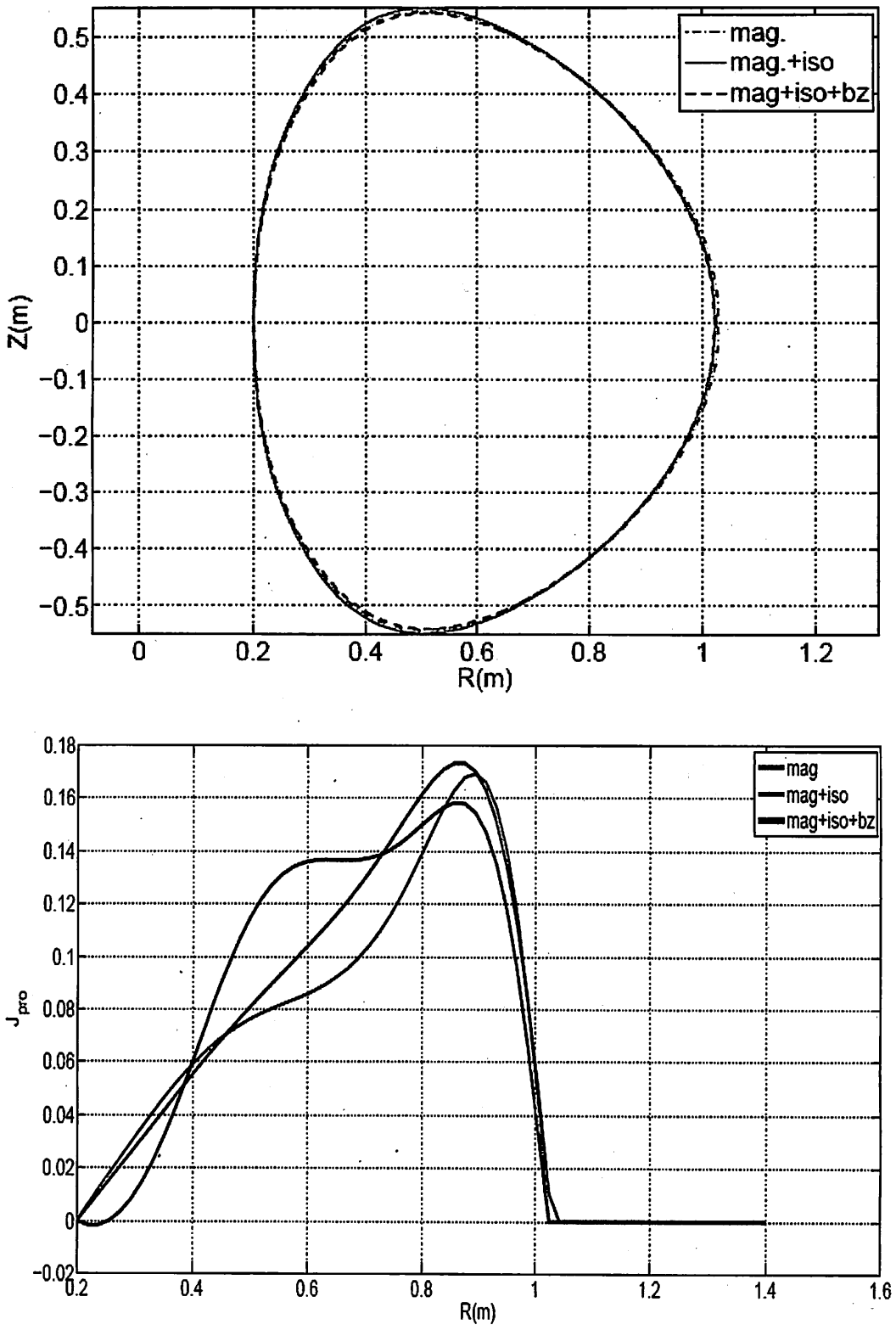

Figure 8 Comparison of reconstructed plasma boundary and current density J.
Note that the reconstruction using {mag}: magnetic data, {mag+iso}: magnetic data + iso-flux constraint and {mag+iso+bz} : magnetic data +iso-flux+ bz constraints.

(Signature) J. Qian

(Name in print) Jinping Qian

国際化推進共同研究概要

No. 6

タイトル; Collaborative Research on QUEST- EBW Current Drive with Divertor, Wall and Recycling Control.

研究代表者 : PENG, Yueng-Kay, Martin

所内世話人 :花田 和明

来訪期間 : 2012年2月20日～21日、24日(途中機関は別途用務)

概要: 共同研究者の Martin Peng 氏は、核融合研究における球状トカマクの利点を提唱し、米国での大型球状トカマク NSTX の概念設計に大きな寄与をした研究者である。QUEST には概念設計時代から、「九大プラズマ境界力学実験装置検討委員会 (核融合科学研究所)」の委員に加わっていただく等、研究の方針について大きな貢献をしていただいた。今回の共同研究は、QUEST の主要な研究課題である、センターソレノイドを用いない電流立ち上げやダイバータ、プラズマ・壁相互作用に関する研究の現状についての議論及び今後の研究方向性についての議論を行なった。また、大学院学生の研究内容にも積極的に助言を与えるなど精力的に共同研究を実施した。今回の訪問で、いくつかの実験提案が行われた。まず、高周波に対する真空容器の Q 値の測定で、これは定量的な評価までは困難であるが、定性的な測定は可能であろうという結論を得て実際に計測を試みることとなった。また、電流の立ち上げについては、高速電子と低温のイオンが共存する系でのポテンシャル計測の重要性が指摘されたがこれは現時点では準備が出来ていないため今後の課題となった。次期の実験期間で中性粒子エネルギー分析を試みることが提案され、現在検討中である。また、Peng 氏から定期的な議論 (1ヶ月に1回程度) を行いたいとの要望があり、これは TV 会議システムでの実施を検討している。

共同研究の最後に、総括的な議論を実施し、現在世界に存在している2大球状トカマクの MAST と NSTX が改造のため数年間止まることが指摘され、今後、QUEST での研究がますます重要になることが指摘された。次年度の共同研究では、球状トカマクでの最重要課題の一つである電流立ち上げについて、高周波を用いた方法に限定してワークショップの開催が提案され、次年度の申請に盛り込まれた。

Form 2

Collaborative Research on QUEST – EBW Current Drive with Divertor, Wall and Recycling Control

2011 collaboration report by YKM Peng, March 2012

Purpose and Background:

The purpose of this collaboration is to develop the physics basis for steady state current drive and PWI/PFC solutions for QUEST, which is also of critical importance to the fusion DEMO.

The QUEST experiment at RIAM has unique and important research goals in Japan and the world fusion research: to produce, test, and understand steady state spherical tokamak (ST) plasmas in the presence of advanced plasma wall and recycling control with improved divertor concepts. Research on QUEST therefore introduces new opportunities, during its Phase II program, to investigate EBW current drive and sustainment of relatively high beta plasmas in concert with strongly expanded divertor configurations and improved plasma edge control. Fusion researchers at ORNL are experienced in RF sources and its utilization on ST experiments, and in boundary physics research on several toroidal experiments. Very recent ORNL initiatives in developing an intense RF plasma source for application to plasma wall interaction (PWI) and plasma facing component (PFC) R&D aim to further strengthen these research capabilities.

As NSTX (PPPL, U.S.) and MAST (CCFE, U.K.) are engaged during 2013-2015 major upgrade activities, QUEST and the accompanying ST experiments, as the largest ST research program in the world, have an opportunity to make large progress in the ST current drive and divertor, wall and recycling control.

Focus of 2011 Collaboration

The 2011 work has been focused on learning details of unique capabilities of the QUEST experiment and its new experimental results in 2011 to achieve the following results:

1) Identify and interpret more clearly the physics features of the new plasma initiated and sustained by ECH/EBW in QUEST, and make initial suggestions of additional measurements and experimental proposals for the experimental campaign in JFY 2012.

2) Based on the improved core plasma description, identify and interpret more clearly the features of plasma and neutrals interactions with the surface materials of the divertor and wall with an aim of improving recycling control.

3) Through more active discussions among ST researchers in Japan, help identify and clarify more clearly additional bi-directional research activities that best enhance the progress of the Japan ST Program.

Highlight of Progress during 2011

1) New results on QUEST from the 2011 experiments were discussed and a number of interesting and potentially important new physics mechanisms were suggested. In the "core plasma" area, the following examples can be noted:

    a. The existence of up to the 3rd harmonic of electron cyclotron resonance may have introduced a new regime of startup and sustainment physics, compared to recent results from LATE and TST-2, which operated so far with up to the 2nd harmonic.

This new physics regime is likely related to the confinement of higher energy electrons (up to 0.5MeV) and the fast ramp-up of the toroidal current (0.3-0.5MA/s) when a constant vertical field is applied.

b. This suggests that the fast electrons initially created near the 1st harmonic only need to be confined (via adjustments to the field decay index) so that their orbits overlap the 2nd harmonic, and so on. This thesis can be modeled to compare with experiments during the next campaign by adjusting the field decay index to allow the startup plasma conditions to revert back to those observed earlier in LATE and TST-2.

c. It is expected that the ion temperatures should be extremely low compared to the electron energies and, due to pitch angle scattering and thermalization of these electrons, likely electron temperature. Such ions could only be confined in the region of closed flux surfaces. Based on reconstructed using approximate current filaments model, the volume of this region is well contained within the volume of toroidal current surfaces largely determined by the phase space distribution of the confined energetic electrons.

d. Assuming relatively prompt "orbit" loss of energetic electrons at a rate much faster than the ion loss rate, it is likely that a large positive potential of the closed flux region plasma is created and maintained. This suggests that an ambipolar potential may be an integral part of the confinement, loss, and stability properties of this plasma system. It will be helpful to measure this potential, as any ion born outside the closed flux surface region would be accelerated toward the wall, gaining the potential energy in the sheath layer as they strike the wall. This may be consistent with the large density of damage sites on the W coupons placed on the vessel wall during the last experiment campaign. These ions could experience charge exchange before striking the wall, allowing energetic neutrals to strike the wall in other areas not dictated by the ion orbits in the presence of strong magnetic and electric field.

e. Due to the very modest plasma densities so far, the ions confined in the region of closed flux surfaces are expected to be dominated by charge-exchange (CX) loss with neutrals that penetrate into that region. These CX neutral would provide a measure of the confined ion temperature. Measurements of the energies and incident angles of these energetic ions and neutrals will shed important light on the mechanisms of ion creation and confinement.

f. It is necessary to have such information to enable appropriate reconstruction of MHD plasma equilibrium, which is expected to be dominated by strongly flowing anisotropic electrons and much colder ions. This would provide increased confidence in the plasma configuration and aid the interpretation of data including particle interactions and recycling with the divertor and wall.

2) With regard to plasma and particle interactions with divertor and wall, the following can be noted:

a. The relatively thick layer of confined energetic electrons is expected to surround the closed flux surface region. This region will affect the particle interactions with the divertor and wall, in addition to the lost energetic electrons.

b. For example, any residual gas from the wall will get most likely become ionized with the electrons falling toward the plasma core and the ions falling toward the wall

in the presence of a strong sheath potential. It is therefore expected that wall fueling would not likely reach the plasma core (the closed flux surface region), leading to very low ion density in the core.

c. Any normal gas puff from the wall would likely lead to little fueling to the plasma core, loss of energetic electron energies and current, and reduction in the ambipolar potential. The behavior of the plasma following a well metered gas puff deserves study to reveal additional properties of this plasma regime.

d. Aside from the strong energetic electron interactions with the divertor and wall, ion and neutral interactions with the these are expected to be rather different from the plasmas in the conventional ST and tokamak regimes (high density, high recycle, high concentrated heat and particle fluxes on divertor surfaces, etc.). Detailed studies of ion and neutral particle incident on the divertor and wall, and their spatial distribution, should be a high priority for this plasma regime.

3) With regard to the broader and related physics issues of interest to this plasma regime, aiming to understand this newly discovered regime for potential fusion applications, the following can be noted:

a. To experimentally understand the limiting processes of this regime of current drive, comparison experiments should be carried out at least with LATE and TST-2.

b. Variations in vertical field decay index in time may lead to additional plasma properties.

c. Additional frequencies in the range of 8 to 28 GHz RF power could be added to introduce additional resonances to within the chamber to produce a wider range of driven electron current properties for measurements.

d. A different way to fuel the plasma core would be needed to enable study of the core plasma ion confinement in the presence of energetic electrons over orbits larger than the core plasma size.

e. Additional diagnostics focusing on this new plasma regime and its special properties may be of interest to a broader interest of the Japan ST research community.

Additional Comments:

1) The opportunity in the next 3-4 year is presented to QUEST and the Japan ST community to make large advances in this new regime of RF driven steady state ST plasma and lead its future research and development for fusion energy and other potential applications.

国際化推進共同研究概要

No. 7

タイトル; Feasibility study for solenoid-less plasma start-up capability in Quest using transient coaxial helicity injection

研究代表者 : Roger Raman

所内世話人 花田 和明

来訪期間 2012 年 3 月 19 日-27 日

概要:現在米国の HIT-II 装置とNSTX装置で得られているTransient Coaxial Helicity Injection (T-CHI)を QUEST に応用すべく概念設計を実施した。QUEST 装置はダイバータ板が既設であること、壁材料が金属であること等、T-CHI におけるメリットが大きく、比較的容易に実験を開始できる可能性がある。一方、QUEST 側ではプラズマ電流の立ち上げは高周波を用いて実現済みであるので、むしろ EBWCD のための周辺領域の密度勾配制御や高密度放電に向けた取り組みに興味がある。これらのことから、T-CHI とSSO-CHI(CHI による定常電流駆動)を並行して検討し、その間にある密度制御をひとつのステップとすることとした。 必要な電極に大きな変更はないが、必要とされる電源は大きく異なる可能性が指摘された。現有の電源でこれらの運転が可能かどうかを今後検討していくと共に、QUEST に導入する際の問題点を今後検討することとなった。

Proposal for Implementing CHI Capability on QUEST

R. Raman, T.R. Jarboe, B.A. Nelson (University of Washington, Seattle, USA)
K. Hanada, H. Zushi, M. Hasegawa, K. Nakamura (Kyushu University, Fukuoka, Japan)
M. Ono (Princeton Plasma Physics Laboratory, Princeton, USA)
M. Nagata (University of Hyogo, Himeji, Japan)

27 March 2012

This proposal is for a US-Japan collaborative research between Kyushu University and the University of Washington for implementing Coaxial Helicity Injection (CHI) [1] capability in the QUEST Spherical Torus at Kyushu University. On QUEST, CHI is capable of playing multiple roles. These include: (1) Generating significant amounts of non-inductively generated closed flux plasma current through the process of *transient* CHI. The level of attained current is expected to be in excess of 100 kA and it would depend on the location of the electrodes and the amount of injector flux that connects the proposed electrodes, subject to the constraint that the injector flux footprints are sufficiently narrow at the injection location. It would provide an alternate solenoid-free generated current for use as a target for the non-inductive startup and sustainment research on QUEST and when coupled to inductive drive, at current levels much higher than what would be possible using induction alone and with hollow current profiles, which may be better targets for sustainment using Electron Bernstein Wave (EBW) current drive. (2) By driving few kA of current along the outer scrape-off-layer (SOL), provide a means to inject density along the SOL and thereby increase the density and vary the density gradient near the separatrix region in support of EBW current drive studies. (3) Develop *steady-state* CHI current drive. The all metal nature of QUEST in addition to its capability for 400 kW of ECH power would both reduce the amount of low-Z impurities initially injected during the application of CHI and because of its ECH heating capability allow a relatively greater fraction of the injected low-Z impurities to burn through radiation barriers, which is necessary for a good confinement discharge. (4) Finally, the multiple electrode configurations would also allow plasma start-up by merging two CHI plasmas injected from either end of the vessel. Such experiments would extend previous work on smaller machines to a very much larger size scale.

I. Implementation of CHI

Installation of CHI capability on QUEST appears to be possible. This document discusses the CHI configuration that could be used to support the four goals noted above.

(A) Transient CHI

On HIT-II and on NSTX, CHI is implemented by driving current along externally produced field lines that connect the inner and outer vacuum vessel components in the presence of externally generated toroidal and poloidal magnetic fields [2-6]. This is qualitatively shown in Figure 1. HIT-II has a major/minor radius of 30/20 cm with a toroidal field at the machine mid-plane of up to 0.5 T, at an elongation of 1.7. The plasma volume is about 0.5 m^3. The outer vessel is fabricated out of 6 mm thick stainless, with the plasma facing side coated with 0.03 mm plasma sprayed tungsten. The inner vessel components including the center stack are fabricated out of 3.5 mm thick stainless steel and a 12.5 mm thick graphite shield covers the plasma facing side. The inner and outer vessel components are electrically insulated from each other using long alumina ceramic insulators located on the high-field side of the machine. NSTX has a major/minor radius of 0.86/0.68 m, a typical plasma volume of 14 m^3 and a maximum plasma elongation of 3. NSTX is designed much like any other tokamak.

The lower divertor plates are used as the injector. All plasma facing components in NSTX are composed of graphite tiles.

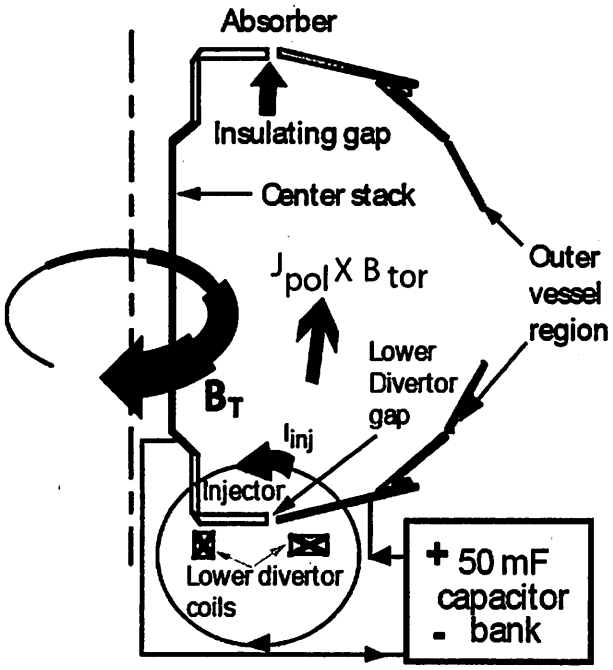

Figure 1: Layout of the transient CHI startup systems in NSTX. The blue circle is the poloidal injector flux produced by the lower divertor coils. This connects the two lower divertor plates, which are insulated. Gas is injected in the region below the divertor gap. On NSTX typically a 5 to 15mF capacitor bank charged up to 1.7kV is used to produce the injector current.

QUEST is intermediate in size. It has a major/minor radius of 0.68/0.4 m, the estimated plasma volume is about 4.5 m^3. Features present on QUEST, that are absent on HIT-II and NSTX are: 1) It is an all metal system, an aspect which is very desirable for the CHI method as low-Z impurities could be reduced to lower levels, 2) It is equipped with a high power Electron Cyclotron Resonance (ECH) heating system that will increase the electron temperature of CHI generated discharges, and thereby further improve their confinement properties.

Because transient CHI discharges do not rely on poloidal flux amplification, the maximum closed poloidal flux in the resulting plasma discharge would be limited by the initial injector flux. Thus, to maximize transient CHI current start-up potential, it is necessary to increase the amount of poloidal flux that connects the CHI electrodes.

Figure 2, shows a set of vacuum field line calculations that are used to calculate the amount of injector flux that could connect both electrodes. In case (a) the QUEST divertor plate which is located at z = -1 m is assumed to stay at that location. The CHI electrodes are assumed to be installed 10 cm above the divertor plate. Energizing the PF5-1 coil at its maximum current limit of 5 kA allows about 4 mWb of poloidal flux to connect the electrodes. CHI plasmas on NSTX typically have a normalized internal inductance of 0.35. Assuming that the location of the CHI plasma major radius is the same as the machine major radius, which is a good approximation for NSTX, the maximum expected closed flux toroidal current for this case would only be 25 kA. Figures (b) and (c) show the effect of the lowering the divertor plates by 10 and 15 cm. In this configuration they are that much closer to the poloidal field coil that generates the injector flux. We find that there is only a small increase in the injector flux, which increases to 5.5 and 6 mWb respectively. The corresponding current generation capability is now 32 and 35 kA respectively. For case (d) we start with case (c) but incline the outer electrode to increase the amount of intersected injector flux. Now, with an additional 2.6 kA driven in the PF5-2 coil, the injector flux increases to 28 mWb, which represents a current generation potential of 160 kA.

For comparison, in Figure 3, we show the case for an idealized configuration, in which the electrode location with respect to the PF coils is further reduced. For this case, with 2 kA in PF5-2 coil (80 kA-Turns or 40% of the full coil current capability) and additional 20 kAmp-

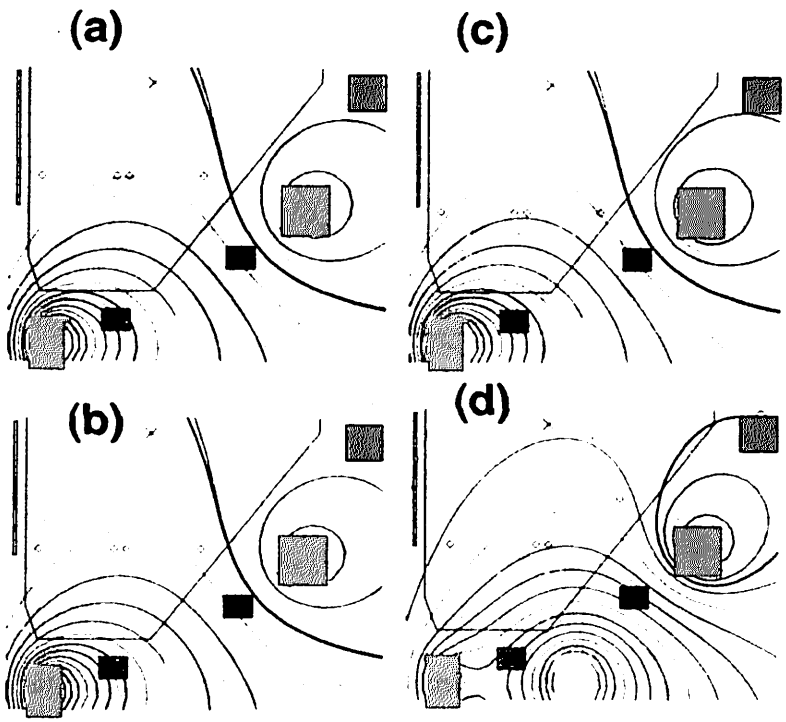

Figure 2: Vacuum field calculations for QUEST to show the benefits of positioning the CHI electrodes closer to the divertor coils. The diamond marks represent the location of the electrodes. The horizontal blue line represents the location of the QUEST divertor plate. Divertor plate at (a) z = -1m. (b) z = -1.1 m, (c) z = -1.15m, (d) z = -1.15 m, but outer electrode is inclined as shown by the two diamond marks.

Turns driven in the adjacent PFLD1 coil (hypothetical shaping coil which does not yet exist) 30 mWb of flux intersects the electrodes resulting in a current generation potential of 175 kA per 2 kA in PF5-2. Implementing this configuration may be difficult for two reasons. First, installation of a continuous toroidal insulator may not be possible. This can be seen from Figure 4, which is a photograph of the region below the divertor plate. The best one could hope to do is to replace the vertical supporting bar with a ceramic bar. In this configuration, especially for the more challenging steady state type discharges, plasma would get into the region below the plates and in the presence of an existing magnetic field provide other paths for the CHI injector current. A continuous toroidal insulator is not possible because of the large port openings on the lower part of the vessel. The presence of several cables below the divertor plate increases the possibility of one or more of the cable's outer conductors providing a current path in the presence of plasma.

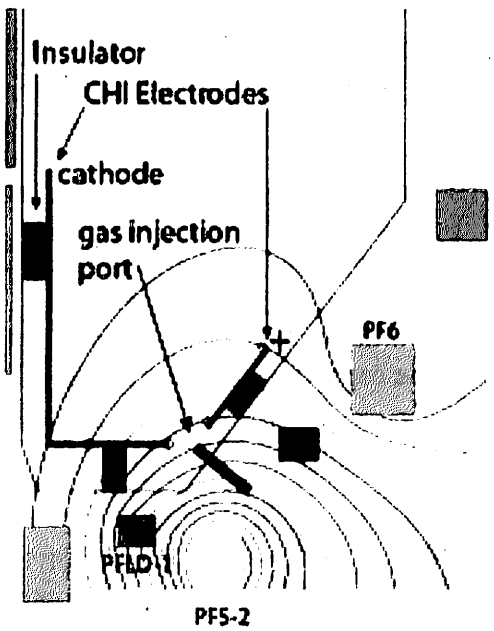

Figure 3: Idealized transient CHI configuration that maximizes the injector flux connecting the electrodes.

A viable method, and one that is also simpler to install is shown in Figure 5. In this configuration the lower divertor plate (shown in Figure 4) is lowered by 15 cm. The electrodes are mounted 8 cm on top of the plate. A continuous toroidal insulator (or if this is not possible a closely coupled toroidal insulator) would be installed as close to the center stack as possible, on top of the divertor plate. This would support the inner CHI electrode, which would be attached to a long cylindrical electrode as shown in Figure 5. Another toroidally continuous insulator would support the outer electrode. The space between both insulators and the electrodes and the divertor

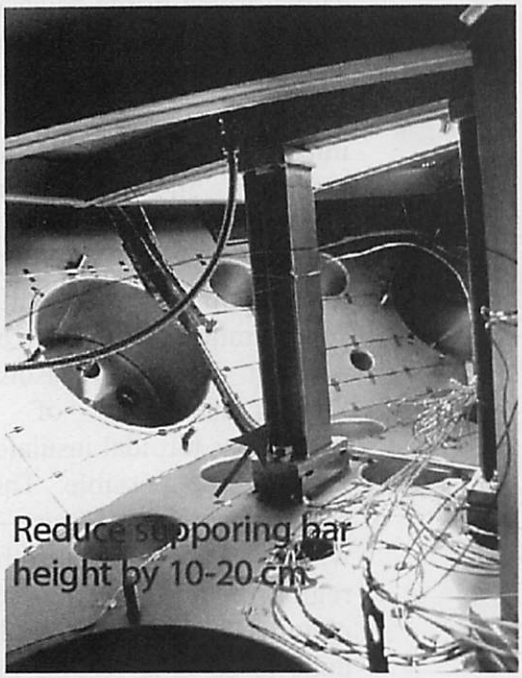

Figure 4: The supporting bar is attached on the top to the divertor plate and at the bottom to the vessel. At least in the lower portion of the vessel that is free of cooling pipes, the height of the supporting bar could be considerably reduced.

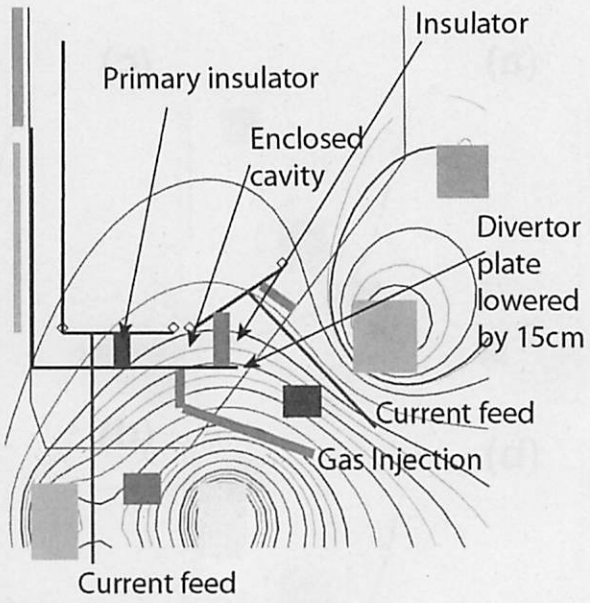

Figure 5: Simpler transient CHI configuration A. The divertor plate is lowerd by 15 cm. The horizontal electrode is mounted 8 cm above the divertor plate using a continuous toroidal insulator. The inclined outer electrode could be supported using insulating bars, in which case an enclosed gas cavity will not form. Such a configuration will require a toroidal gas manifold below the gap region. In this configuration both the inner and outer plates are floating and are not electrically connected to the vessel, so the current path is much better defined.

plate would form a natural cavity into which gas would be injected, much as it is done on NSTX. The electrodes would be fabricated out of stainless steel or inconel and coated with high-quality tungsten or preferably bonded to a thin tungsten or molybdenum plate. If tungsten coating is used, it should be carried out in a vacuum chamber so that the coated tungsten does not get oxidized. Otherwise the benefits QUEST offers (non-carbon, i.e. metallic components) would not be adequately realized.

Table 1 shows the calculated parameters for transient CHI for nominal operating conditions on HIT-II, NSTX and projected values for QUEST. To inject about 28 mWb of flux minimum injector currents of about 12 kA would be required by the CHI power supply. This can be provided by a 30 kJ capacitor bank with a capacitance of 2.5 mF and operated at 5 kV. The total system inductance and resistance needs to be on the order of 80 μH and 80 mOhms or less. To be conservative a bank with approximately twice the capacitance is prefereed.

(B) Edge Biasing Experiments

Much of the work for this was done on DIII-D [7-8] and in other tokamak. This involves positioning the outer strike point of a pre-existing diverted plasma discharge on the outer electrode, shown in Figure 5 and biasing this electrode with respect to the inner electrode. The direction of the E x B drift determines if the SOL density would increase or decrease. Here E is the applied electric field. The normal configuration would have the inner electrode

be the cathode and the outer electrode or the vessel the ground. Because the DC rectifier supply may require a hard ground, the outer electrode may need to be grounded to the vessel. For the current in the toroidal field coil center leg pointed in the downward direction, the E x $B_{toroidal}$ drift would be into the vessel, as it would be for normal CHI operation. The plasma drift into the vessel would be directed along the outer SOL, which should then also contribute to an increase in electron density inside the separatrix. These results are well described in the papers by M.J. Schaffer [7-8]. DIII-D results suggest that voltages on the order of 200 V and injected currents on the order of 5 kA are needed for substantial changes to the neutral pressure in the private flux region and average electron density inside the plasma. The DIII-D results do not report the electron density profile near the SOL for such experiments, but it must also increase. The rectifier power supply requirements are a voltage capability of 400 V and current capability of >5kA (2 MW power supply).

Parameters	HIT-II	NSTX	QUEST
Major Radius: R_o [m]	0.3	0.86	0.68
Minor radius: a [m]	0.2	0.66	0.40
TF rod current: I_{TF} [MA]	0.8	2.4	1.7
Toroidal Field: B_T [T]	0.5	0.55	0.50
Toroidal Flux: ϕ_T [Wb]	0.2	2.5	0.78
Plasma normalized inductance: *li*	0.35	0.35	0.35
Nominal plasma inductance: Lp [μH]	0.07	0.19	0.15
Injector flux footprint: d [m]	0.1	0.6	0.25
Nominal Injector flux: ψ_{inj} [mWb]	8	47	28
Nominal Start-up current: I_p [MA]	0.1	0.25	0.15
Bubble burst current * 1.2 : Iinj [kA]	14	4	11.3
Current Multiplication: Flux ratio	7	50	28
Max Injector flux: [mWb]	16	80	28-60

Table 1: Representative parameters for transient CHI start-up on HIT-II, NSTX and QUEST

(C) Pulsed CHI and Steady-State CHI

The electrode configuration for this mode of operation has two possibilities. In the first, preferred mode of operation, only the inner 'L-shaped' section shown in Configuration A is required. The outer electrode is not required. Additionally and armor could be added near the outer wall, as shown in Figure 6. This is referred to, as Configuration B. Switching from Configuration A to B would require shorting out the outer electrode to the vessel. For this configuration, it is necessary that a region of open flux be present between the center stack

and the plasma. Currents would be driven from the lower electrode to the upper electrode (or vise versa) through the inner open field line region (as described in the Reference by Jarboe [9]). HIT-II discharges that exhibited the best flux amplification factors operated in this mode and are described in the paper by Redd [10]. The advantage of this method is that helicity would flow from the high-field side region to the low field side region that now contains the main plasma discharge.

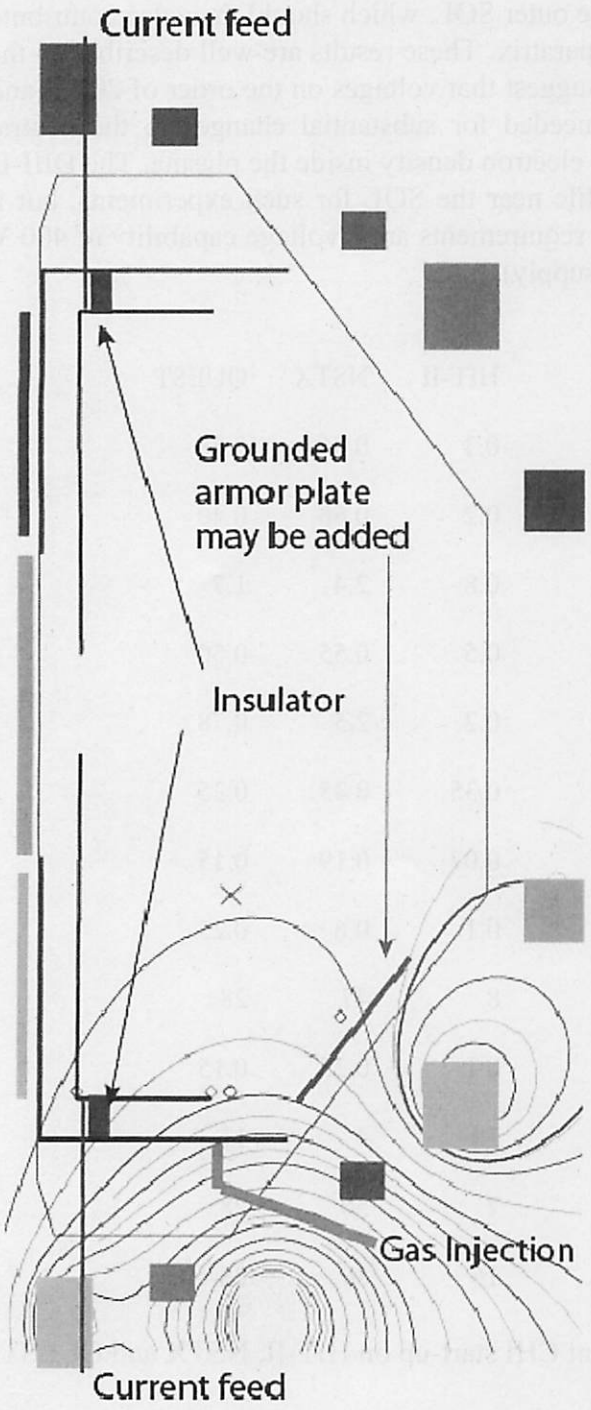

Figure 6: Preferred Configuration B for steady-state CHI. The current is driven along the open field lines on the inner portion of the machine, between the two inner electrodes.

An alternate method for SS CHI would be to use configuration A and drive current from the outer electrode to the inner electrode. Here, because helicity is injected along the low field side region, penetration efficiency into the main plasma discharge that is now located in regions of higher field is expected to be less.

During the pulsed CHI mode of operation, either Configuration B or A would be used and the CHI system pulsed for several ms to compensate for droops in plasma current. In support of steady-state CHI such short duration pulsed experiments wiould likely be conducted, perhaps initially using a capacitor bank system. Eventually after good confinement discharges are demonstrated using the steady-state CHI approach, they could form the basis for a plasma current feedback control system.

Based on NSTX experience a 1 kV, >10 kA supply (10 MW) is needed. Initial work could begin with existing power supplies, such as the HF and SN supplies at QUEST. The HF supply in the pulsed mode is capable of operation at up to 2 kV and 12 kA of injected current, which is adequate to conduct the initial experiments.

(E) CHI Merging Experiments

This is not a primary focus for the near term, so it is not described in any detail. Here we simply note that transient CHI plasmas could be injected from both ends of the machine, using two transient CHI power supplies. The merged plasma would be hotter

due to field line reconnection. The experiments are similar in nature to the work conducted at the Univ. of Tokyo [11] and at PPPL [12], but on a much larger size scale.

II. Gas Injection System

Figure 7 describes the required gas injection system. It would consist of a pizeo valve to provide steady state gas flow that would be needed for the SS CHI experiments and for the edge biasing experiments and a pulsed valve to rapidly inject on the order of 2 Torr.L of gas within a few ms for transient CHI. The system is based on what was used on HIT-II and presently in use on NSTX.

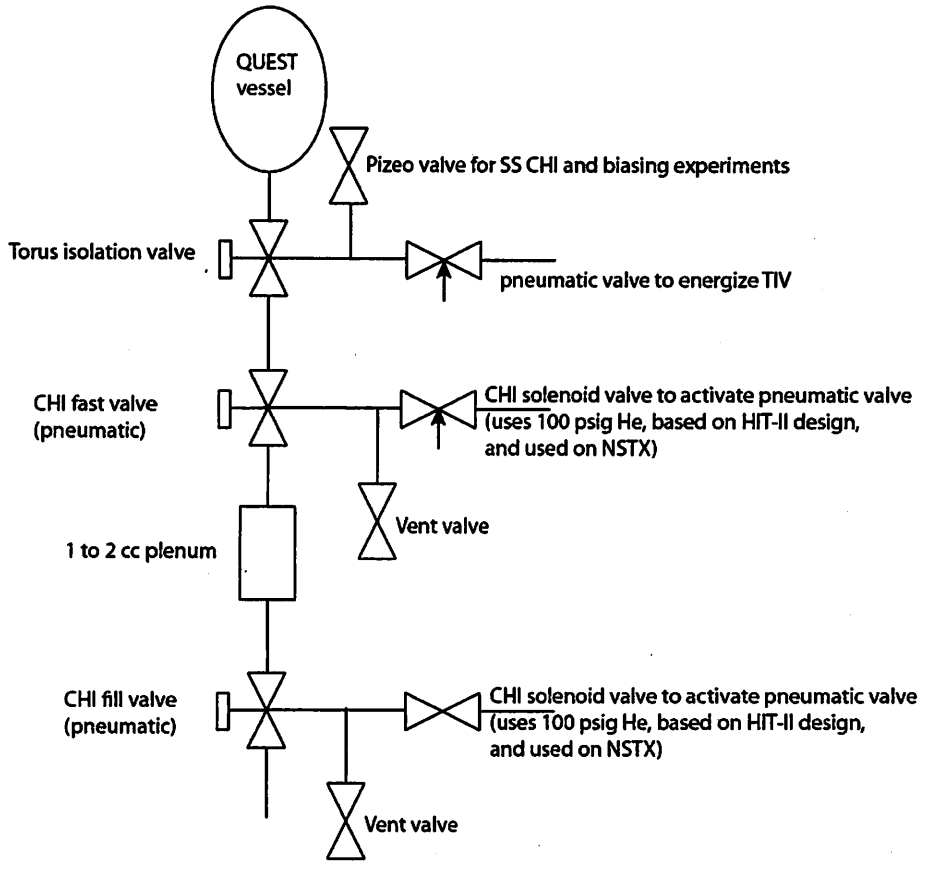

Figure 7: CHI gas injection system for QUEST is based on HIT-II and NSTX configurations.

III. Preliminary Estimates of Cost

The cost estimates are quite preliminary, as a detailed engineering design of the system is yet to be conducted. The cost is based on prior experience in fabricating components of this size.

Internal hardware [$180k]
–Shorten divertor support: 1.5 man weeks + materials ($20k)
–Fabricate L-shaped assembly (probably in two half circles): 3 man weeks + materials ($50k)
–Outer target plate: 2 man weeks + materials: $30k

–Primary insulator (continuous or close interlocking sections): $30k
–Outer insulator bars: $10k
–Outer insulator if installed as a continuous section: $40k

Gas injection system [$20k]
–Cost for pizeo valves, pneumatic valves, solenoid valves and piping and assembly

Capacitor bank system [$200k]
–US$150k – 500k, cost depends on use of existing parts and company that fabricates it
–Univ. of Washington has expertise assembling such systems

DC power supplies [$50k]
–It is assumed that initial experiments would start with existing supplies
–Estimate $50k for small modifications to existing QUEST power supplies

Current feed connections [$50k]
–Requires and is dependent on engineering analysis
–Depends on number and location of current feeds (4 feeds preferred for each electrode)

Cost summary

Power systems:	$250k
Current feeds:	$50k
Vessel hardware:	$180k
Gas systems:	$20k
Initial total:	$500k
Engineering analysis:	$50k
Total:	**$550k**

The critical components are the insulators and the current feeds. The cost assumes that the insulator would be fabricated as a single toroidal section, as this is the ideal preferred configuration. Fabricating the insulator as shorter toroidal segments that interlock may be an alternate possibility. This would reduce the cost. Both options should be studied as part of the detailed engineering study.

IV. Required Next Steps

As a next step it is necessary to arrive at a reference design that includes dimensions for the different components. Issues related to electrical feed through connections need to be resolved. A design for the ceramic insulator needs to worked out and sent to insulator manufacturers for price quotes. After that a design review needs to be held with broader participation to iron out any missing details. Since numerous experiments are possible, there should be a prioritization for the goals and level of effort and commitment of collaborators (NSTX, U-Washington and other groups within Japan).

V. Summary and Conclusion

Numerous experiments are possible as reflected by the collaborator interests listed below.

NSTX
–Transient CHI is of primary interest
–Experiments on QUEST would benefit NSTX plasma start-up and sustainment program (near-term)

University of Washington
–Interested in developing steady-state CHI
–Also interested in transient CHI on QUEST
–Merging reconnection of two plasmoids for plasma start-up (very long-term)

QUEST
–Short-term goal is to control edge density in support of EBW experiments
–Mid-term goal is pulsed steady-state CHI for feedback control on plasma current
–Long-term goal is steady-state CHI development

A CHI design that is flexible would allow many of these ideas to be tested and further developed on QUEST.

A possible path forward may be as described below.

Transient CHI (Start with this)
–This is well-demonstrated, low risk for QUEST
–CHI + OH will quickly enhance QUEST steady-state current drive program
–Because the CHI injector current pulse is very short (< 2 ms), it allows the CHI hardware to be tested and if necessary improved before driving current for long periods of time as required by the other two systems

Edge density control (Simultaneously start this, but this may take longer)
–Needs some development because CHI has not been used for this purpose before
–Need to ensure insulators are capable of holding off >400V for long durations during the presence of plasma

Steady-State CHI (This is a long-term project)
–Potential for fundamental new results (with good confinement)
–Requires considerable development and would benefit from prior work on edge density control. Impurity control will be extremely important for the realization of discharges with good plasma confinement.

–Need to ensure insulators are capable of holding off ~1 kV for long durations under the presence of plasma while the power supply injects > 10 kA

Recommendations

1. The lower divertor plate should be lowered as much as possible. This not only increases the transient CHI current potential in QUEST, but it would also make it much easier for the divertor coils to control the equilibrium of normal elongated discharges on QUEST. Consider lowering it by as much as 25 cm.
2. If the main CHI electrodes serve as divertor plates, the lower divertor plate could be much thinner as its purpose now would be simply to protect and shield the components below this plate from plasma and undesirable arcing.
3. Impurity control is crucial to realize the benefits of steady state CHI. This involves using electrode materials that are largely free of metal oxides as well as in carefully determining the lowest injector current that generates useful plasma current with good confinement properties. ECH on QUEST would clearly help in this regard. If plasma sprayed tungsten is used, unless adequate care is taken, the bonded tungsten granules may be oxidized. Simply cleaning the surface, such as for instance with high power CHI discharges or glow discharge cleaning may not be adequate. With bonded metal only the surface may be oxidized and this could be cleaned using plasma discharges.
4. Electrode materials should be thoroughly washed ultrasonically in oil removing solvents and baked prior to installation.
5. Desirable to obtain cost estimates for both high-quality tungsten coating and for a thin tungsten or molybdenum plate bonded to stainless steel or inconel electrodes.
6. The cost of the insulator could vary by a large factor. This depends on the quality of the insulator material as well as on size. A full continuous toroidal insulator is desired – if possible.

References

1] T.R. Jarboe, Formation and steady-state sustainment of a tokamak by coaxial helicity injection, Fusion Technology, **15**, 7 (1989)

[2] R. Raman, D. Mueller, T.R. Jarboe, B.A. Nelson, M.G. Bell, S. Gerhardt, B. LeBlanc, J. Menard, M. Ono, L. Rouquomore, V. Soukhanovskii, Experimental demonstration of tokamak inductive flux saving by transient coaxial helicity injection in national spherical torus experiment, Physics of Plasmas **18**, 092504 (2011)

[3] R. Raman, S.C. Jardin, J. Menard, T.R. Jarboe, M.G. Bell, D. Mueller, B.A. Nelson, M. Ono, Transient CHI start-up simulations with the TSC, Nuclear Fusion **51**, 113018 (2011)

[4] R. Raman, D. Mueller, B.A. Nelson, T.R. Jarboe, S.Gerhardt, H.W. Kugel, B. LeBlanc, R. Maingi, J. Menard, M. Ono, S. Paul, L. Roquemore, S. Sabbagh, V. Soukhanovskii, Demonstration of Tokamak Ohmic Flux Savings using Transient Coaxial Helicity Injection in NSTX, Phys. Rev. Lett., **104**, 095003 (2010)

[5] R. Raman, B.A. Nelson, M.G. Bell, T.R. Jarboe, D. Mueller, T. Bigelow, B. LeBlanc, R. Maqueda, J. Menard, M. Ono, R. Wilson, Efficient generation of closed magnetic flux surfaces in a large spherical tokamak using coaxial helicity injection, Phys. Rev. Lett., **97**, 175002 (2006)

[6] R. Raman, T.R. Jarboe, B.A. Nelson, V.A. Izzo, R.G. O'Neill, A.J. Redd, R.J. Smith, Demonstration of plasma start-up by coaxial helicity injection, Phys. Rev. Lett., **90**, 075005 (2003)

[7] M.J. Schaffer, et al., Effect of divertor bias on plasma flow in the DIII-D scrape-off layer, Nuclear Fusion **32**, (1992) 855

[8] M.J. Schaffer, et al., Increased divertor exhaust by electrical bias in DIII-D, Nuclear Fusion **36**, (1996) 495

[9] T.R. Jarboe, An explanation of closed-flux formation and sustainment using coaxial helicity injection on HIT-II, Plasma. Phys. Control. Fusion **52** (2010) 045001

[10] A.J. Redd, et al., Flux amplification in Helicity Injected Torus (HIT-II) coaxial helicity injection discharges, Phys. Plasmas **15**, 022506 (2008)

[11] Y. Ono, M. Inomoto, T. Okazaki and Y. Ueda, Experimental Investigation of Three-Component Magnetic Reconnection by Use of Merging Spheromaks and Tokamaks, Physics of Plasmas, Vol. 4, No. 5, Pt. 2, (1997), 1953.

[12] M. Yamada, Y. Ono, A. Hayakawa, and M. Katsurai, Phys. Rev. Lett. **65**, 721(1990)

国際化推進共同研究概要

No. 8

タイトル;Pilot design of ECH/ECCD transmission line for Alcator C-mod

研究代表者 : Wukitch, Stephan(白岩俊一 氏 PSFC,MIT)

所内世話人 花田 和明

来訪期間 2011 年 12 月 2 日

概要:Alcator C-mod でのECHシステムの導入計画に合わせて TRIAM-1M で開発された remote steering アンテナを応用したアンテナを Alcator C-mod に設置することが可能かどうかの議論を行なった。また、Alcator C-mod で開発された full wave の低域混成波解析コードをQUESTで実施しているEBWCDに関する理論計算について適応するための議論を行った。

Pilot design of ECH/ECCD transmission line for Alcator C-Mod

S. Wukitch, O. Meneghini, and S. Shiraiwa

PSFC, MIT, Cambridge, MA, 02139, USA

The result of joint activity to assess the feasibility of ECH/ECCD on Alcator C-Mod is presented. Alcator C-Mod is a compact (R~0.7m) high field (Bt = 4~8T) tokamak, and is suitable for testing the wave physics using the parameters exactly envisioned on ITER. C-Mod is equipped with 3 MW (source power, is being upgraded to 4MW) LHCD and ICRF heating for auxiliary heating. However, LHCD profile tends to be far off-axis (as discussed below in detail), while FWCD depends strongly on the electron beta, which motivated us to consider ECH/ECCD as a tool for central current drive and instability control. Furthermore, this would enable studies on the synergy between EC and LH waves.

One of issues on implementing ECH/ECCD on C-Mod is its strong limited access to the vacuum ports. The horizontal ports have a straight section of about 2 m with the opening of 30cm x 60cm. Also, they are crowded by various diagnostics and heating systems. In such a circumstance, the remote-steering mirror system developed on TRIAM-1M could be a good choice for the ECH launcher. For the first year activity, we have focused on wave modeling simulations using GENRAY/CQL3D code [4, 5].

1. Target plasma for ECH

Alcator C-Mod is equipped with 4.6 GHz LHCD system for off-axis current drive. So far, up-to 1.2 MW of microwave power has been injected to plasmas. Weakly reversed shear plasmas have been sustained fully non-inductively at n_0 of 8 x 10^{19} m^{-3}[1], which is close to what is envisioned in ITER stead state scenarios. Presently, an additional off-midplane launcher (LH3) is under fabrication and its installation is planned for this fall. Recent LHCD modeling using a ray-tracing code predicts that the combination of LH3 together with the existing LH2

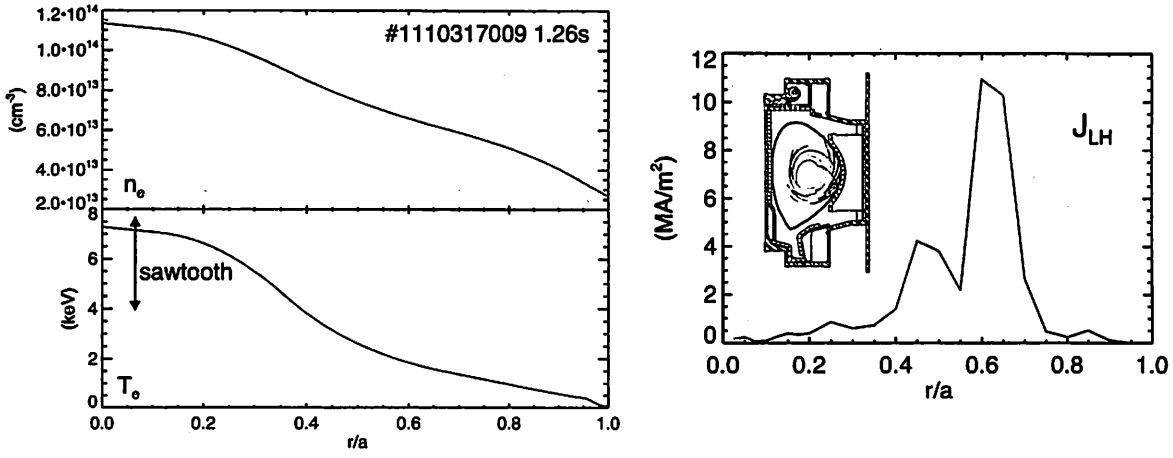

Fig 1: Ray-tracing calculation of LHCD in an I-mode plasma. (right) density and temperature profile of #1110317009 discharge at 1.26s. (left) the predicted LH driven current profile and ray-trajectories projected on the poloidal cross-section. Color of ray indicate the normalized ray power.

improves the power absorption significantly due to the velocity space synergy [2]. With a high Te target plasma, most of the power is absorbed during the first pass (single pass absorption regime). Consequently, the driven current is expected to be localized around r/a of 0.5 to 0.7. Figure 1 shows an example such a simulation using I-mode target plasma [3]. In this case, LHCD was localized around r/a~0.6 and the total LH current is about 0.5 MA, while the target plasma current is 0.7 MA.

2. ECCD simulation using GENRAY/CQL3D

The microwave power source considered in this scope study is E3980 Gyrotron manufactured by TOSHIBA (500 KW at 168 GHz). This frequency corresponds to the fundamental EC frequency at 6T and very close to what is planned on ITER. NIFS, which used 6 of these tubes for the LHD experiment, kindly agreed to lease three of these tubes.

In order to calculate the ECCD deposition and driven current GENRAY/CQL3D ray-tracing Fokker-Planck package was used. Figure 2 shows the results of these simulations. The ECH launcher was assumed to be installed below the LH3 launcher and the launched poloidal angle was swept to adjust the power deposition profile. The largest driven current is obtained in the case of on-axis CD. Total current of 60-170kA are large enough to control the q-profile near the magnetic axis.

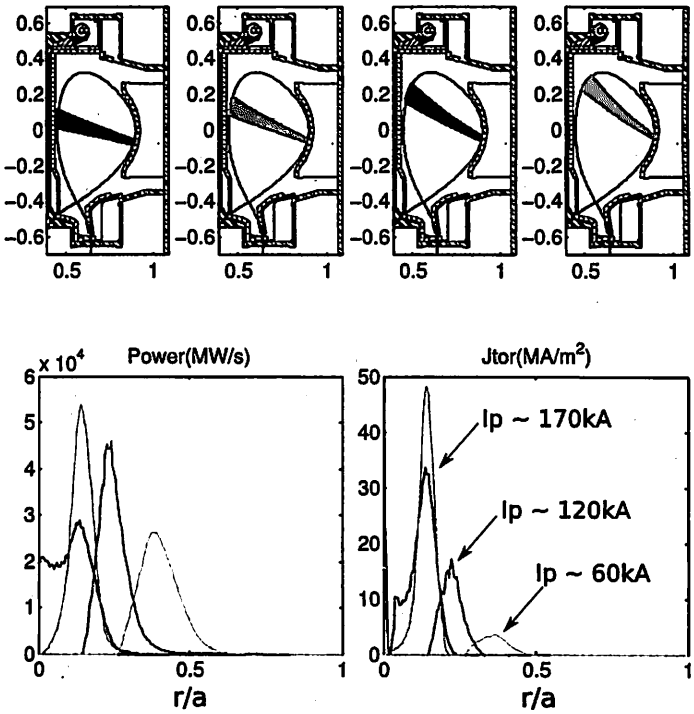

Fig 2: ECCD simulations on Alcator C-Mod using GENRAY/CQL3D. The microwave power of 1MW was launched as O-mode with 20 deg. in the toroidal direction and in different poloidal angles.

3. Summary

A scope study of ECH/ECCD on Alcator C-Mod has been performed using the GENRAY/CQL3D ray-tracing Fokker-Planck package, and good core current driven is predicted. Presently, LH waves and EC waves are simulated independently. Further studies are necessary to investigate the impact of the interaction of these waves, which has not yet been fully explored experimentally.

References

[1] S. Shiraiwa *et al Nucl. Fusion*, **51**, 103024 (2011)
[2] I. Fidone et al., Phys. Fluids, **27**, 2468 (1984)
[3] D.G. Whyte *et al Nucl. Fusion*, **50**, 105005 (2010)
[4] A.P. Smirnov, et al., Bull Amer. Phys. Soc. 39, 1626 (1994).
[5] R.W. Harvey and M.G. McCoy, Proc. IAEA TCM on Advances in Sim. and Modeling of Thermonuclear Plasmas, Montreal, 527 (1992), available through USDOC/NTIS No. DE93002962.

国際化推進共同研究概要

No. 9

タイトル： Effects of tansmutant helium on the microstructure of fusion reactor structural materials.

研究代表者：ODETTE, George, Robert

所内世話人：渡辺　英雄

期　間：　2011年11月12日～11月23日

核融合炉構造材料の損傷評価には核変換により形成されるヘリウムとははじきだし量(dpa)との関連が重要である。本研究は、ＵＣＳＢが保有する各種の材料にたいして、九州大学・応用力学研究所が所有するタンデム照射を用いて照射実験を実施した。また、得られた重畳効果に関しては、他の照射施設での実験も含めて詳細に検討された。

Effects of tansmutant helium on the microstructure of fusion reactor structural materials

G. R. Odette and T. Yamamoto (University of California Santa Barbara), H. Watanabe (Kyushu University)

Introduction

One of the challenges that fusion reactor materials development faces is to manage and mitigate the possible effects of transmutation He on the mechanical properties of first wall structural materials. In a typical DEMO fusion reactor design, after a year of operation at a neutron wall load of 5 MW/m^2 ≈ 500 appm He will be generated in Fe-based materials as well as displacement damage of ≈ 50 dpa. Helium bubbles form in the matrix as well as on dislocations, precipitate interfaces and grain boundaries (GB) [1]. Based on a physically motivated analysis of limited data in the literature for fracture toughness transition temperature shifts (ΔT), we previously proposed a model that predicts that irradiation hardening ($\Delta\sigma_y$) coupled with GB He embrittlement of tempered martensitic steels (TMS) produces very large ΔT at low irradiation temperatures [2,3]. Figure 1 shows examples of the predictions for neutron and spallation proton (STIP) irradiation conditions, plotted with more recent data, indicating that the model predicted extraordinary ΔT up to > 500 °C after STIP irradiation to ≈ 2000 appm He at ≈ 20 dpa [4].

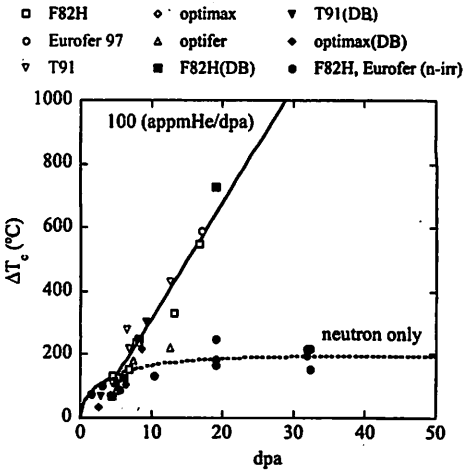

Figure 1 Model prediction and experimental data for the DBTT shift due to irradiation with and without He accumulation in tempered martensitic steels for fusion reactors[4].

The fundamental overriding questions about He-dpa synergisms include: a) What are the basic interacting mechanisms controlling He and defect transport, fate and consequences, and how are they influenced by the starting microstructure and irradiation variables (dpa rate, He/dpa ratio, temperature and applied stress); and, b) how can the detrimental effects of He-dpa synergisms be mitigated and managed by proper microstructural design?

Our approach to answering these questions is to build experimental knowledge base through the experiments in wide ranges of material and environmental variables, that is coordinated with development of physically based models of the microstructural evolution. The objective of this research is to examine He behavior in the materials irradiated in the High Energy Ion Generating Apparatus (HEIGA) of RIAM, that provides experimental data for very higher He-to-damage ratio. We have laid out the details of the experiments in this new joint research to investigate He/dpa ratio, dpa and dpa rate efficiently.

Experimental techniques to study He-dpa synergisms

We have previously demonstrated that in situ He implantation (ISHI) in mixed spectrum fission reactor irradiations provides a very attractive approach to assessing the effects of He-dpa synergisms, while avoiding most of the confounding effects associated with Ni- or B-doping type experiments [1,5-9]. The technique can generally probe the He/dpa range of 10 to 60 appm at a damage level higher than 5 dpa at damage rate of ≈ 10^{-6} dpa/s. Another approach is to use spallation proton irradiation such as STIP, spallation target irradiation program. A high energy (≈ 600MeV) proton beam produces significant amount of He as well as displacement damage in target materials generally at a rate from 50 to 100 appm He/dpa for damage levels > 5 dpa. Heavy ion (such as Fe^{3+}) beam irradiation is also widely used to produce displacement damages in materials. In dual or triple ion (DI, TI) beam facilities, an additional use of a He ion beam can produce He/dpa up to ≈ 100 appm/dpa. Single ion irradiation of He can implant a large amount of He while introducing relatively small amount of displacement damages, which results in very high He/dpa ratio up to ≈10^4 appm. These various He implantation techniques are summarized in Figure 2 in terms of the He/dpa and dpa conditions typically available. The figure also shows actual irradiation conditions in our recent experiments including a plan for 3MeV He^{2+} irradiation in HEIGA. The three lines in the figure indicate iso-He concentration at levels of 100, 500 and 2000 appm He. By comparing microstructural evolution in HEIGA irradiated sample with that in our recent STIP, DuET and ISHI experiments, we can investigate the effects of He/dpa rate at a similar amount of implanted He.

Damage rate effects

Figure 2 also shows that the ISHI in test reactors and DI techniques have a wide overlap in the He/dpa – dose scheme, while the heavy ion irradiation utilized in DI generally produces damages at very high rates from

10^{-4} to 10^{-3} dpa/s. It is two to three orders of magnitude higher than that in the test reactors. The typical DEMO condition (50 dpa annually, or > 1.6 x 10^{-6} dpa/s) is found between those two techniques, a little bit higher than that in the test reactors. Thus we also will include the effects of the damage rate in our models.

The HEIGA can create He/dpa ratio of 50 appm in the depth range of 2 to 3 μm from the surface at a dpa rate of ≈ 10^{-6} dpa/s. It will allow us to examine the initial stage of He accumulation at the dose rate similar to HFIR ISHI experiments. DuET irradiation can also create similar He/dpa and dpa conditions while it is at much higher dose rate ≈ 10^{-4} dpa/s, that enables us to examine the dose rate effects as well.

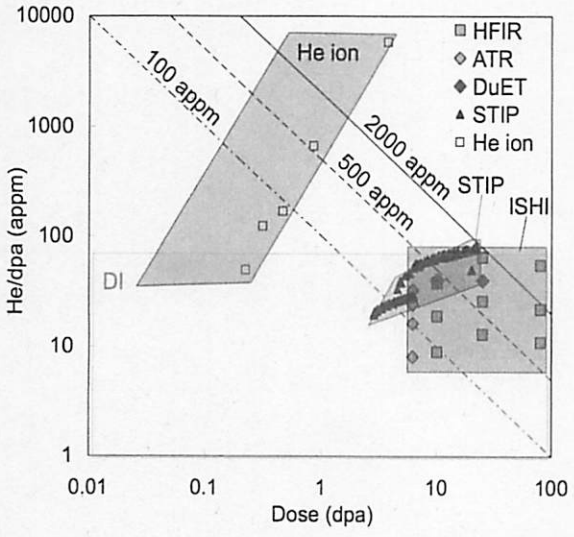

Figure 2 Typical range of He/dpa and dpa for various He implantation techniques (boxes) with our recent experimental conditions (dots).

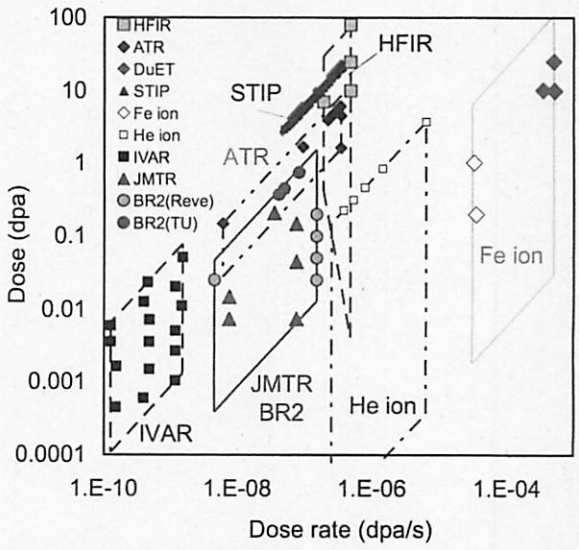

Figure 3 Typical ranges of dose and dose rate for various irradiation techniques (boxes) with our recent experimental conditions (dots).

Irradiation Plan and microstructure analytical tools

We will irradiate tempered martensitic steels such as F82H and Eurofer 97, and nanostructure ferritic alloys such as MA957 and Fe-14%Cr-1%W-0.25%Y-0.1%Ti, and Fe-Cr model alloys with He ion beam in HEIGA, followed by microstructure observation in TEM. Irradiation will be performed to the peak He levels from ≈ 5000 to 50000 appm at the peak dpa levels of 0.4 to 4 dpa, respectively, in the temperature range from 300 to 650 °C. TEM samples will be prepared using the focus ion beam (FIB) micromachining by picking up selected parts of the irradiated specimens or using an electro-polishing technique. We will also examine thermal desorption spectra of implanted He, that provide useful information on defect-He interaction.

References:

1. Y. Dai, G. R. Odettte, T. Yamamoto, *The Effects of helium on irradiated structural alloys* in: R.J.M. Konings(ed.) Comprehensive Nuclear Materials, volume 1, pp. 141-193 Amsterdam: Elsevier (2012)
2. T. Yamamoto, G.R. Odette, H. Kishimoto, J-W. Rensman, P. Miao, J. Nucl. Mater. **356** (2006) 27.
3. G.R. Odette, T. Yamamoto, H.J. Rathbun, M.Y. He, M.L. Hribernik, J.W. Rensman, J. Nucl. Mater. **323** (2003) 313.
4. T. Yamamoto,Y. Dai, G. R. Odette, M. Salston, P. Miao, Trans. American Nuclear Society, 98 (2008) 1111.
5. T. Yamamoto, G. R. Odette, L. R. Greenwood, Fusion Materials Semiannual Report 1/1 to 6/30/2005 DOE/ER-313/38 (2005) 95.
6. T. Yamamoto, G.R. Odette, P. Miao, D. T. Hoelzer, J. Bentley, N. Hashimoto, H. Tanigawa, R. J. Kurtz, J. Nucl. Mater., 367 (2007) 399.
7. G.R. Odette, M.J. Alinger, and B.D.Wirth, Annu. Rev. Mater. Res. 38 (2008)471.
8. G.R. Odette, P. Miao, D.J. Edwards, T. Yamamoto, R. J. Kurtz, Y. Tanigawa, J. Nucl. Mat. 417 (2011) 1001.
9. T. Yamamoto, G.R. Odette, P. Miao, D. J. Edwards, R. J. Kurtz., J. Nucl. Mater., 386-388 (2009) 338.